BBA - Molecular Cell Research 1870 (2023) 119526

Contents lists available at ScienceDirect

BBA - Molecular Cell Research

journal homepage: www.elsevier.com/locate/bbamcr

Research Paper

Stability of Rad51 recombinase and persistence of Rad51 DNA repair foci depends on post-translational modifiers, ubiquitin and SUMO

Justyna Antoniuk-Majchrzak [a,1], Tuguldur Enkhbaatar [a,1], Anna Długajczyk [a], Joanna Kaminska [a], Marek Skoneczny [a], Daniel J. Klionsky [b], Adrianna Skoneczna [a,*]

[a] Institute of Biochemistry and Biophysics, Polish Academy of Sciences, Warsaw 02-106, Poland
[b] Life Sciences Institute, Department of Molecular, Cellular, and Developmental Biology, University of Michigan, Ann Arbor, MI 48109, USA

ARTICLE INFO

Keywords:
DNA damage response
DSB repair
Genome instability
Homologous recombination
Proteasome
SUMOylation
Ubiquitination

ABSTRACT

The DNA double-strand breaks are particularly deleterious, especially when an error-free repair pathway is unavailable, enforcing the error-prone recombination pathways to repair the lesion. Cells can resume the cell cycle but at the expense of decreased viability due to genome rearrangements. One of the major players involved in recombinational repair of DNA damage is Rad51 recombinase, a protein responsible for presynaptic complex formation. We previously showed that an increased level of this protein promotes the usage of illegitimate recombination. Here we show that the level of Rad51 is regulated via the ubiquitin-dependent proteolytic pathway. The ubiquitination of Rad51 depends on multiple E3 enzymes, including SUMO-targeted ubiquitin ligases. We also demonstrate that Rad51 can be modified by both ubiquitin and SUMO. Moreover, its modification with ubiquitin may lead to opposite effects: degradation dependent on Rad6, Rad18, Slx8, Dia2, and the anaphase-promoting complex, or stabilization dependent on Rsp5. We also show that post-translational modifications with SUMO and ubiquitin affect Rad51's ability to form and disassemble DNA repair foci, respectively, influencing cell cycle progression and cell viability in genotoxic stress conditions. Our data suggest the existence of a complex E3 ligases network that regulates Rad51 recombinase's turnover, its molecular activity, and access to DNA, limiting it to the proportions optimal for the actual cell cycle stage and growth conditions, e.g., stress. Dysregulation of this network would result in a drop in cell viability due to uncontrolled genome rearrangement in the yeast cells. In mammals would promote the development of genetic diseases and cancer.

1. Introduction

The maintenance of genetic information is essential for cells but not easy to achieve due to constant environmental and metabolic threats. Particularly deleterious for genome integrity are stresses causing double-strand breaks in DNA because this type of damage may lead to DNA rearrangements or loss of parts of chromosomes. To avoid such scenarios and restore vital genetic information, the repair pathways evolved, reassuring the re-connection of the broken DNA strands. In the yeast *Saccharomyces cerevisiae*, the most accurate repair pathway dedicated to double-strand break (DSB) repair is homologous recombination (HR). One of the proteins essential for this repair is Rad51, a protein belonging to the RecA family of recombinases [1]. Due to its capacity to bind single- and double-stranded DNA, DNA-dependent ATPase activity, ability to form a filament on DNA, and feedback interactions with various proteins engaged in DNA repair (Rad54, Rad52, Sgs1, replication protein A [RPA complex], etc.), the recombinase Rad51 executes the critical early step of homologous recombination: the search for homologous DNA to serve as a template during the repair of DSBs [2–6]. Numerous lines of evidence substantiate the essentiality of the function performed by this protein. Orthologs of the yeast *RAD51* gene have been identified in various organisms, including humans [7], and *rad51* mutants display replication defects and chromosomal instability both in yeast and human cells [8,9]. In vertebrates, the absence of Rad51 leads to embryonic lethality [10]. Moreover, mutations in human RAD51 are linked to breast cancer [11,12] and Fanconi anemia (complementation group R, FANCR) [13,14].

Rad51 is involved in mitotic and meiotic recombination; however, its role is slightly different in each process. Because the Rad51 homolog Dmc1 is present during meiosis, the proteins share their responsibilities.

* Corresponding author at: Institute of Biochemistry and Biophysics, Polish Academy of Sciences, Pawińskiego 5A, 02-106 Warsaw, Poland.
E-mail address: ada@ibb.waw.pl (A. Skoneczna).
[1] These authors contributed to the work equally.

https://doi.org/10.1016/j.bbamcr.2023.119526
Received 24 March 2023; Received in revised form 2 June 2023; Accepted 19 June 2023
Available online 24 June 2023

While Dmc1 is responsible for interhomolog recombination, Rad51 promotes Dmc1 presynaptic filament assembly and participates in intersister repair, leading to non-crossover products [15], [16,17].

Rad51 activity is regulated on several levels. Besides interactions with DNA and various DNA repair proteins, Rad51 activity depends on post-translational modifications (PTMs), e.g., phosphorylation. The Cdc28-dependent phosphorylation of Ser125 and Ser375 at the G_2/M border of the cell cycle promotes the DNA binding affinity of Rad51 [18]. In turn, Mec1-dependent phosphorylation on the Ser192 residue is required for two functions of Rad51: DNA-binding and ATPase activity [19]. The abundance of Rad51 in the cell also influences its function. The availability of Rad51 is determined by the level of expression of the *RAD51* gene, which increases in a cell cycle-dependent manner during G1/S transition and after exposure to genotoxic stress when demand for Rad51 protein increases [20,21]. The abundance of Rad51 in the cell strongly depends on its half-life, which should be tightly controlled to regulate and resume the homologous recombination repair pathway. Indeed, the high level of Rad51 during replication stress leads to an increased usage of illegitimate recombination causing frequent genome rearrangement [22].

In this study we demonstrated that Rad51 protein level is controlled by proteolytic digestion. Its half-life changes in response to environmental conditions, e.g., upon genotoxic stress. We also identified several ubiquitin-conjugating enzymes (E2), ubiquitin ligases (E3) and SUMO (E3) ligases affecting the Rad51 cellular level. We showed that Rad51 is post-translationally modified by ubiquitin (Ub) and SUMO. Interestingly, different patterns of Rad51 ubiquitination and SUMOylation were visible in various conditions. Our results indicate that the proteolytic pathway controls the Rad51 level in the cell in a Ub- and SUMO-dependent manner. A range of factors is involved in the regulation of this process, signifying the need for precise Rad51 regulation. We also showed that PTMs of Rad51 recombinase influence its ability to form DNA repair foci, suggesting a role of these modifications in recruiting Rad51 to the damage site in the DNA and releasing it from the DNA after the repair was completed.

2. Materials and methods

2.1. Strains and plasmids

Most of the strains used in this study (Table A.1) are in the BY4741 (*Mat a his3Δ1 leu2Δ0 met15Δ0 ura3Δ0*) and WCG4a (*MAT*a *ura3 leu2–3112 his3–11,15 rad5–535 Can^S GAL2*) background. The deletion constructs in the BY4741 background came from the yeast knockout collection (Open Biosystems), and were initially prepared during the *Saccharomyces* genome deletion project [23]. Strains carrying point mutations affecting essential genes in the BY4741 background came from a yeast temperature-sensitive mutant collection [24]. Strain YAD11 was constructed by gene replacement of the *SIZ1* gene by a *siz1::hphMX6* cassette, amplified using siz1up and siz1lw primers (Table A.2) and genomic DNA isolated from the YAH144 [25] strain as a template, in the BY4741 *nfi1/siz2Δ* strain, using a standard in vivo recombination method. Strains YAM7 and YAM8 were created by introduction of the *rad18::LEU2* and *rad18::URA3* cassettes to the BY4741 *slx8Δ* strain, respectively. The *rad18::LEU2* cassette was obtained from a PCR reaction using RAD18up and RAD18lw primers and YAS33 [26] strain genomic DNA as template. The *rad18::URA3* cassette was obtained in a PCR reaction using RAD18kup and RAD18klw primers and pRS316 [27] DNA as template. Strain YAM19 was created by introduction of the *rad18::URA3* cassettes to the BY4741 *dia2Δ* strain. Strain YAM9 was prepared by replacement of the *ULP2* gene by a *ulp2::natNT2* cassette, amplified using ULP2kup and ULP2klw primers (Table A.2) and pRS41N plasmid DNA [28] (Table A.3) as a template, in the BY4741 strain, using a standard in vivo recombination method. Strains YJK1 and YJK2 are WCG4a and YWH24 derivatives, respectively, in which the *TRP1* gene was replaced with *trp1::kanMX4* by marker swap using the pM3925 [29] vector. Strain YAS27 is a BY4741 derivative obtained by introducing into the genome the *GAL1pRAD18* fusion at the *RAD18* locus. For this purpose, the YIp211-GALpRAD18 [30] plasmid digested with *Sal*I was used. The correctness of the resulting strain was proved by PCR using GAL1A and RAD18lw primers.

Plasmid pCM188-SIZ1 was made by PCR amplification of the DNA fragment carrying the *SIZ1* ORF with SIZpup and SIZ1n-lw primers and BY4741 genomic DNA as a template and cloning into the pCM188 [31] vector digested with *Pme*I. Plasmid pRS413-RAD51 was made by removing the *ClaI-PstI* fragment, carrying the 3′-terminal part of the *RAD51-YFP* gene fusion, from the pRS413-PRO-RAD51-GFP [19] plasmid, and replacing it with the *ClaI-PstI* fragment, carrying the 3′-terminal part of the native *RAD51* gene with its natural terminator, obtained in the PCR using BY4741 genomic DNA using primers RAD51up and RAD51L-PstI.

2.2. Culture media and growth conditions

YPD medium contained 1 % yeast extract (Difco, Mt. Pritchard, NSW, Australia), 2 % bactopeptone (Difco) and 2 % glucose (POCh, Gliwice, Poland). YPGal was made the same as YPD, except that galactose was used instead of glucose. SC medium contained 0.67 % yeast nitrogen base (Difco) and 2 % glucose and was supplemented with all amino acids, uracil and adenine (Formedium, Hunstanton, UK). The solid medium also contained 2.5 % agar (Difco). Liquid cultures were grown with agitation at ~200 r.p.m. (New Brunswick Scientific, Edison, NJ); the temperature sensitive mutants were grown at 23 °C, and other strains at 28 °C.

2.3. Determination of protein half-life

Yeast cells were grown at 28 °C in YPD medium to a density of 5×10^7 cells/ml. Then, the culture was divided into three parts. The first part was treated with 0.03 % MMS (Merck), the second with zeocin (Invivogen; 50 mg/ml final concentration), and the third part was the non-treated control. After 90 min of incubation at 28 °C cycloheximide (Sigma, St. Louis, MO, USA; 0.5 mg/ml final concentration) was added. Culture samples were harvested at different time-points after treatment. Then, the level of protein in the sample was determined by western blot (WB). Three independent biological repetitions of this experiment were performed.

2.4. Protein analysis

For WB, cells were grown to the exponential phase (5×10^6 cells/ml) in YPD medium at appropriate temperature with shaking. Then, 1×10^8 cells were collected by centrifugation and proteins were extracted using the NaOH-TCA method. Samples were suspended in Laemmli sample buffer supplemented with a protease and phosphatase inhibitor cocktail (PIC; 1 mM PMSF, cOmplete™ Protease Inhibitor Cocktail [Roche, Basel, Switzerland], PhosSTOP [Roche, Basel, Switzerland]), and 10 mM N-ethyl maleimide (Sigma, St. Louis, MO, USA). Samples were vigorously vortexed and frozen in liquid nitrogen. Immediately before use, the samples were boiled for 5 min. After centrifugation (19,300 *g* for 2 min), equal volumes of the cell extracts were separated by SDS-PAGE (7 % or 8 % polyacrylamide gel, depending on the mass of the analyzed protein), and the proteins transferred onto PVDF membrane (Amersham, Germany). Blots were blocked for 2 h in 5 % (w:v) nonfat-dried milk and/or 3 % (w:v) BSA in TBST (25 mM Tris-HCl, pH 7.5, 137 mM NaCl, 27 mM KCl, 0.1 % [v:v] Tween-20) before probing with primary antibodies. Rad51 protein was detected by incubating the membranes with rabbit polyclonal antibody anti-Rad51 (1:2000, Thermo Fisher Scientific, Cat# PA5–34905, RRID:AB_2552256) followed by incubation with goat anti-rabbit IgG conjugated to horseradish peroxidase (HRP; 1:2000, Agilent, Cat# P0448, RRID:AB_2617138). Ub was detected using mouse monoclonal anti-Ub antibody (1:500, Santa Cruz

Biotechnology, Cat# sc-8017, RRID:AB_628423), yeast SUMO was detected with rabbit polyclonal anti-Smt3 antibody (1:1000, Abcam, Cat# ab14405, RRID:AB_301186), followed by incubation with goat anti-mouse IgG conjugated to HRP (1:2000, Agilent, Cat# P0447, RRID: AB_2617137) or goat anti-rabbit IgG conjugated to HRP (1:2000, Agilent, Cat# P0448, RRID:AB_2617138), respectively. For normalization of signals, we used actin or Pgk1, which was detected by using mouse anti-actin monoclonal antibody (1:5000, Millipore, Cat# MAB1501, RRID:AB_2223041) or mouse anti-Pgk1 antibody (1:10000, Abcam, Cat# ab113687, RRID:AB_10861977), respectively, followed by goat anti-mouse IgG (H + L) alkaline phosphatase (AP)-conjugated (1:3000, Bio-Rad, Cat# 170–6520, RRID:AB_11125348) antibody or Alexa Fluor 546 goat anti-mouse IgG (H + L) (1:3000, Thermo Fisher Scientific, Cat# A-11030, RRID:AB_2534089). Immunoreactive proteins on the blots were visualized using chemiluminescent substrates: SuperSignal WestPico (Pierce) for HRP and CDP Star, ready-to-use (Roche, Basel, Switzerland) for AP and documented with a charge-coupled device camera (FluorChem Q Multi Image III, Alpha Innotech, San Leandro, CA). The results from independent experiments were averaged to determine the relative protein levels. The resulting bands were quantified by using Image Quant 5.2 (Molecular Dynamics, Inc., Sunnyvale, CA). The protein level was normalized to that of Act1, Pgk1 or to total proteins detected with Ponceau S staining.

2.5. Affinity-isolation assay

The affinity isolation of His6-tagged ubiquitinated and His6-tagged SUMOylated Rad51 was performed in two biological replicates, as described previously [32]. The strains in the WCG4a background (YJK1 and YJK2) were transformed with the plasmids YEp96-6His-Ubi [33], YEp112 [*UBI-HA*] or YEp96 empty vector [34]. The strains in the BY4741 background were transformed with the plasmids YEp181-CUP1-His-Smt3 [35], YEp181-CUP1-His-Ubi or YEp181 empty vector [36]. Transformants were grown to exponential phase (5×10^6 cells/ml) at 28 °C with shaking in appropriate synthetic selective media. Then, $CuSO_4$ was added to a final concentration of 100 μM and cells were cultivated for an additional 4 h. The same number of cells (10^9) from each culture was harvested and disrupted with glass beads in a lysis buffer (100 mM NaPi, pH 8, 10 mM Tris, pH 8, 6 M guanidine, 5 mM imidazole, 10 mM β-mercaptoethanol, 0.1 % Triton X-100). The lysate was incubated with Ni^{2+}-NTA beads (Ni-NTA Superflow, Qiagen) for 2 h at room temperature with rocking, and washed first with lysis buffer and, then with washing buffer (100 mM NaPi, pH 6.4, 10 mM Tris, pH 6.4, 8 M urea, 10 mM mercaptoethanol, 0.1 % Triton X-100). The fraction of proteins bound to the Ni^{2+}-NTA beads was recovered by boiling in a Laemmli sample buffer (0.2 M Tris, pH 6.8, 8 % SDS, 20 % β-mercaptoethanol, 40 % glycerol, 0.02 % [w:v] bromophenol blue) containing 6 M urea. All buffers, except the latter were supplemented with cOmplete™ protease inhibitor (Roche), and N-ethylmaleimide (NEM; SIGMA). The total lysate and Ni^{2+}-NTA resin-bound proteins and non-bound supernatants were separated by SDS-PAGE and analyzed by WB with anti-Rad51 antibody.

2.6. Immunoprecipitation

Yeast strains from the moveable ORF (MORF) collection carrying individual plasmids of interest with genes under the control of the *GAL1p* promoter were grown on selective medium SC-URA + 2 % glucose at an appropriate temperature with shaking to the exponential phase (5×10^6 cells/ml). Then cells were collected by centrifugation at 1600 *g* for 3 min, washed with YNB medium, suspended in SC-URA + 2 % galactose, and allowed to grow for an additional 4 h to induce the *GAL1p* promoter. Next, 1×10^9 cells were collected by centrifugation at 1600 *g* for 3 min, and proteins were extracted in 700 μl of RIPA buffer (150 mM NaCl, 50 mM Tris, pH 7.4, 1 % Nonidet P-40, 0.5 % sodium deoxycholate, 0.1 % SDS supplemented with PIC and 1 mM Na_3VO_4) using the glass beads method. After centrifugation at 16000 *g* for 10 min at 4 °C, the protein extract was transferred to a new tube. A portion of the extract was mixed with a 4 x Laemmli sample buffer (0.2 M Tris, pH 6.8, 8 % SDS, 20 % β-mercaptoethanol, 40 % glycerol, 0.02 % [w:v] bromophenol blue) for control of protein levels in the total extract. The immunoprecipitation was performed for 1 h at 4 °C with rotation using 500 μl of protein extract, 300 μl of WASH buffer (150 mM NaCl, 50 mM Tris, pH 7.5 supplemented with PIC and 1 mM Na_3VO_4) and 50 μl of rabbit anti-Rad51 antibody (Thermo Fisher Scientific, PA5–34905, RRID:AB_2552256) covalently linked to the magnetic agarose resin (CNBr-activated StepFast MAG, Bio Toolomics Ltd. Consett, County Durham, UK) according to the supplier's protocol. After incubation, the resins were washed three times with 1 ml of WASH buffer using a magnetic rack for resin separation. Finally, the immunoprecipitated proteins were suspended in 90 μl of 1.5 x Laemmli sample buffer supplemented with PIC and 1 mM Na_3VO_4). Samples were frozen in liquid nitrogen and stored at −70 °C until further usage. Prior to SDS-PAGE, samples were heated at 99 °C for 5 min in a heat block. After SDS-PAGE, wet transfer in Towbin buffer (25 mM Tris base, 192 mM glycine) was performed overnight at 4 °C on a PVDF membrane (Amersham). The western hybridization with appropriate antibodies was then performed.

2.7. Determination of Rad51 foci frequency and foci intensity by fluorescence microscopy

The W4121—20D strain [37] carrying a *YFP-RAD51* gene fusion in the genome was transformed with pYES2 (empty vector) or selected plasmids from the MORF collection [38], i. e. pMMS21, pRSP5, and pSLX8 carrying the analyzed genes under *GAL1p* promoter control. Obtained transformants were grown overnight to the exponential phase (1×10^7 cells/ml) in SC-URA liquid medium at 28 °C with shaking. Cells were then washed with SC medium, suspended in liquid media SC-URA + 2 % galactose, and incubated for another 4 h to allow expression from the *GAL1p* promoter. In the cultures intended for treatment with the genotoxic agent zeocin (InvivoGen), after 3 h of galactose induction, SC liquid medium was changed to rich YP medium +2 % galactose and zeocin added to a final concentration of 100 μg/ml, then cells were cultivated for another 1 h. The media change was needed because zeocin is ineffective in the minimal medium. After induction, cells were washed with phosphate-buffered saline (PBS) and placed on microscope slides. Imaging was performed using a Zeiss AxioCam MRc5 Digital Camera, mounted on a Zeiss Axio Imager.M2 fluorescence microscope operated by Zeiss Axio Vision 4.8 software with the following exposure times: DIC (200 ms) and YFP-Rad51 (3200 ms). All images were acquired at 100-fold magnification using a Zeiss EC Plan-NEOFLUAR 100×/1.3 NA objective lens. The YFP-Rad51 signal was visualized using the Zeiss 38 HE GFP Filter set. Data from 2 independent biological replicates with at least 300 cells in each of them were counted for each data point. The number of foci was counted using a combination of several image processing programs. Binary masks of cells were obtained through Cellpose (RRID:SCR_021716, [39]) software. Binary masks of Rad51 foci were created by image preprocessing in Fiji (RRID:SCR_002285, [40]) with the plugin MorphoLibJ [41]. Processed images were used to generate probability masks using semantic segmentation in ilastik (RRID: SCR_015246, [42]) and finally using CellProfiler Image Analysis Software (RRID:SCR_007358, [43]) for counting occurrences of foci in the areas of individual cells. Foci intensities were calculated by converting foci binary masks to regions of interest in Fiji software and calculating the mean integrated density value for each set of raw images. Data for all foci were counted for each strain and condition. Statistical significance was calculated using the Mann-Whitney test.

Data acquisition and statistical analysis were performed in Jupyter Notebook (RRID:SCR_018315, [44]) using Pandas (RRID:SCR_018214, [45]) and SciPy (RRID:SCR_008058, [46]) libraries.

2.8. Sensitivity drop assay

To estimate the level of sensitivity of yeast cells to genotoxic stress, we performed a semi-quantitative drop-assay as described previously [47], with some modifications. To get an insight into possible linkage between observed phenotype, overproduction of E3 ligases, and Rad51 we performed a complementation assay, using BY4741 *rad51Δ* cells transformed with a plasmid selected from the MORF collection in parallel with the pRS413 or pRS413-RAD51 plasmid. Each transformant was grown in the selection condition (SC-URA-HIS+2 % glucose) with shaking at 28 °C to a density of approximately 1–2 × 10^7 cells per ml, then the carbon source in the medium was changed to 2 % galactose to induce expression from *GAL1p* promoter. After 4 h of incubation, cells were collected by centrifugation, washed with sterile water, and adjusted to a density of 3.3 × 10^7 cells per ml via resuspension in water. Cells were then sequentially diluted at a 1:6 ratio and 3.3-µl drops of each dilution was spotted onto Omnitray (Nunc, Roskilde, Denmark) plates containing YP medium +2 % galactose +0.01 % glucose or the same medium supplemented with 15 µg/ml zeocin (InvivoGen), 50 mM hydroxyurea (HU; Sigma) or 0.01 % methyl methanesulfonate (MMS; Merck). The plates were then incubated at 28 °C for 2 days. The zeocin sensitivity tests plates were also kept in the dark because of the zeocin light-sensitivity. The plate images were digitized with a flat-bed scanner (Epson Perfection V370 Photo). All tests were performed in duplicate.

2.9. Visualization of DAPI-stained nuclear DNA by fluorescence microscopy

The BY4741 *rad51Δ* strain transformed with the pRS413 empty vector or pRAD51, and one of the plasmids from the MORF collection (pMMS21, pRSP5, pSLX8, or pYES2 [control]) was grown overnight to the exponential phase (10^7 cells/ml) in SC-URA-HIS +2 % glucose liquid medium at 28 °C with shaking. Then, strains were incubated for 4 h in SC-URA-HIS +2 % galactose liquid medium for *GAL1p* promoter induction. The staining procedure was as in [22] with slight modifications. Briefly, after incubation, the cells were centrifuged (800 *g* in a microcentrifuge) and then permeabilized and fixed in 1 ml of 80 % ethanol (Polmos, Warsaw, Poland) for 15 min. Permeabilized cells were then pelleted by centrifugation (800 *g*), resuspended in PBS with 1 µg/ml 4′,6-diamidino-2-phenylindole (DAPI; Invitrogen) and incubated for 15 min in the dark at room temperature. After DAPI staining, cells were washed twice with 1 ml of PBS, suspended in 50 µl PBS and placed on a microscope slide. Imaging was performed using the same microscope, camera, and software setup as for the Rad51 foci analysis, and Zeiss 49 DAPI Filter Set. Exposure times for DIC and DAPI channels were as follows: 200 ms and 175 ms, respectively.

2.10. DNA content analysis by flow cytometry

The DNA content of yeast cells was measured by flow cytometry as previously described [48], with some modifications. The subject of analysis were strains transformed with two plasmids, one from the MORF collection (carrying an E3 ligase encoding gene or control vector) and pRAD51 or empty vector control (pRS413). Analyzed strains were cultivated at 28 °C with shaking in the selective media SC-URA-HIS +2 % glucose to the exponential phase (1 × 10^7 cells/ml), then the glucose in the media was replaced with galactose to induce expression from the *GAL1p* promoter. After 4-h incubation, about 1 × 10^7 cells/ml were collected by centrifugation (19,300 *g* for 1 min) and subjected to permeabilization and fixation via suspension in 1 ml of chilled (−20 °C) 80 % ethanol. The suspensions were held at room temperature for at least 2 h. The fixed cells were washed twice using FACS buffer (0.2 M Tris-HCl [Sigma-Aldrich] pH 7.4 and 20 mM EDTA [Merck, Darmstadt, Germany]). To remove the RNA, cells suspensions were incubated in FACS buffer with 1 mg/ml RNase A (Sigma-Aldrich) for 2 h at 37 °C. The cells were then washed with PBS, stained with 100 µl of propidium iodide solution (50 µg/ml in PBS; Calbiochem) overnight at 4 °C in the dark, and diluted with 900 µl of PBS. Before flow cytometry analysis, the cells were sonicated three times for 10 s in a Branson 2800 ultrasonic bath, to avoid cell clumping. The analysis of the DNA content was performed with a FACSCalibur analyzer (Becton-Dickinson, Franklin Lakes, NJ). A total of 10,000 cells in each sample were counted.

3. Results

3.1. Rad51 protein level in the cell is actively regulated via Ub-dependent proteolysis

One of the ways to regulate protein functioning in the cell is to control its abundance, and the fastest way to do this is to alter the rate of proteolysis, limiting degradation when the protein is needed. We asked if the half-life of Rad51 is changed under genotoxic stress conditions when there is a higher demand for its activity. Accordingly, we analyzed the stability of Rad51, following the addition of cycloheximide (CHX) to inhibit protein translation. We found that Rad51 degradation displayed a steady rate of turnover in the wild-type strain following treatment with CHX (Fig. 1 a, b, NT). When cells were additionally treated with MMS or zeocin to induce DNA damage the degradation of Rad51 was reduced. The results suggested that Rad51 degradation is actively regulated in response to DNA damage.

Cells wield multiple proteolytic systems to carry out protein degradation. One of the most common pathways used for this purpose is Ub-dependent proteolysis via the 26S proteasome. To answer the question of whether Rad51 is a substrate for the proteasome, we measured the steady-state level of Rad51 in yeast mutants defective in various proteasomal activities. We exploited the *pre2-K108R*, *pre3-T20A*, and *pup1-T30A* mutant strains, where chymotrypsin-like, trypsin-like, and peptidyl-glutamyl peptide-hydrolyzing (PHGH) activities of 20S proteasome core were inactivated, respectively [49]. In proteasome mutant strains there was an increased level of Rad51 (Fig. 1 c). A similar effect was visible in *ump1Δ* cells lacking proteasome maturase [51]. We therefore concluded that Rad51 is degraded by the proteasome.

The proteins that undergo proteasomal degradation first have to be tagged with Ub. Thus, we took advantage of the His-tagged Ub system to check whether Rad51 is modified by Ub. Using Ni^{2+}-NTA sepharose, we purified ubiquitinated proteins from the strains carrying a plasmid expressing a His-tagged Ub variant under the control of the inducible *CUP1* promoter [33]. The Ni^{2+}-NTA-bound fraction of proteins, i.e., proteins modified with Ub, and total cell extract, were then separated by SDS-PAGE and analyzed by WB. As shown on the left panel of Fig. 1 d, the total extracts from *pre2–1* mutant cells contain greater amounts of high molecular mass forms of Rad51, presumably poly-ubiquitinated, compared to the wild-type cells. The image on the right side of this figure, showing the immunodetection of Rad51 in samples of His-ubiquitinated proteins purified on Ni^{2+}-NTA resin from the total extracts of the same cells, confirms that those high molecular mass forms of Rad51 are indeed poly-ubiquitinated.

3.2. Multiple E2 and E3 enzymes participate in the in vivo degradation of Rad51

Because Rad51 is poly-ubiquitinated, and we found increased levels of Rad51 in the strains lacking enzymes involved in protein ubiquitination (Fig. 1 c), we asked which E2 and E3 enzymes are responsible for that modification. To answer this question, we first performed in silico studies. We searched the *Saccharomyces* Genome Database (SGD) (RRID: SCR_004694) looking for proteins responsible for proteolysis or contributing to its regulation. In addition, we explored the *RAD51* dataset deposited in the Biological General Repository for Interaction Datasets (BioGRID) (RRID:SCR_007393), looking for Rad51 interactors. Then, we compared the two obtained datasets; overlapping candidates were examined further. We employed WB to examine the effect of null or

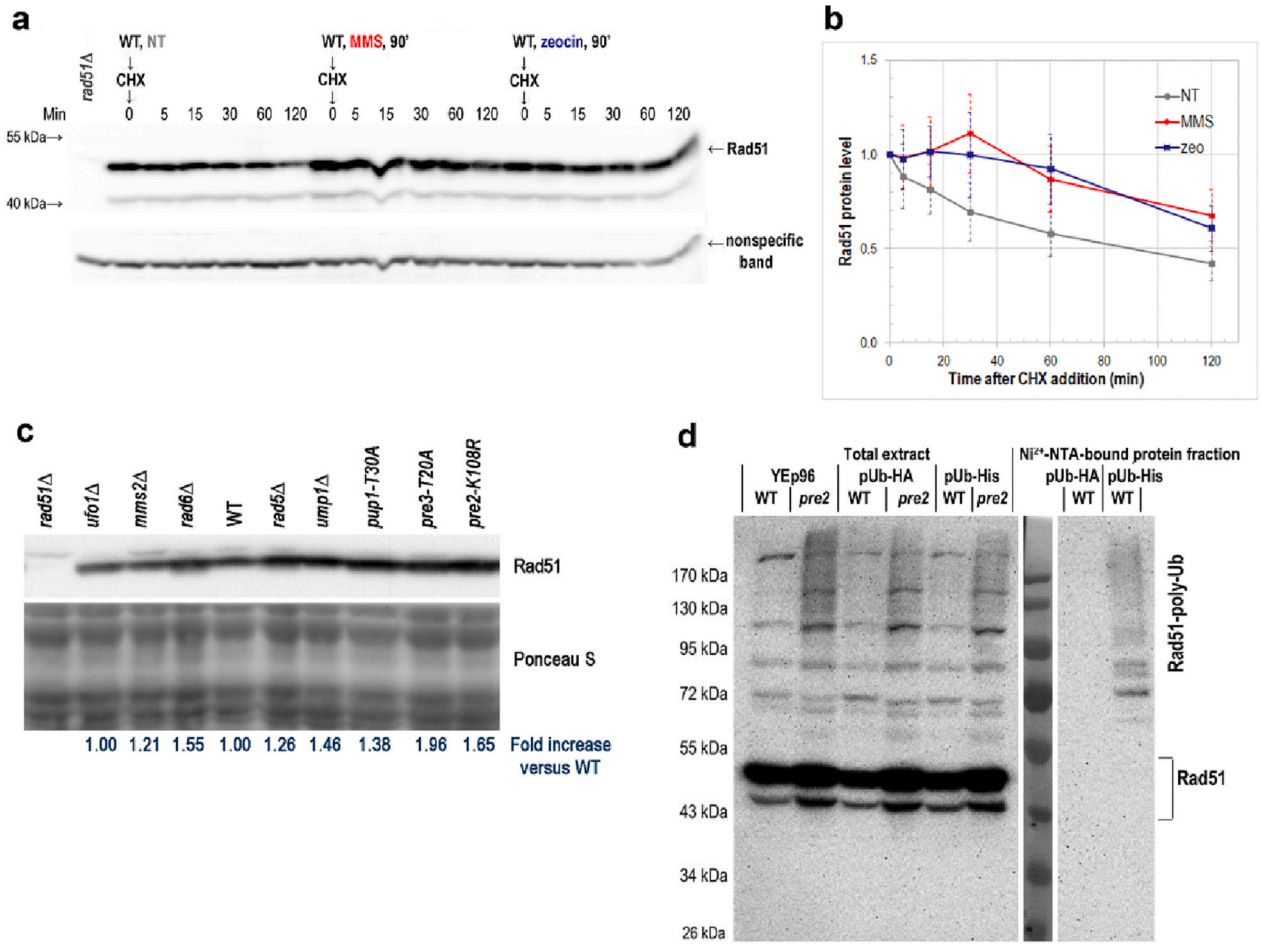

Fig. 1. The Rad51 protein level is regulated by Ub-dependent proteolysis.
(a) Rad51 stability is changed after genotoxic stress. A culture of the WT strain (BY4741) was divided into three parts: control (NT), treated with 0.03 % MMS (MMS), and treated with 50 mg/ml zeocin (zeo). After 90 min of incubation, cycloheximide (CHX) was added to a final concentration of 0.5 mg/ml. Protein samples were harvested at the indicated time points, and immunoblotting was performed. The immunoblotting results of one representative experiment are shown in (a). Averaged quantitative data of band intensities from three independent biological repetitions are plotted in (b). Error bars represent standard deviation. (c) The steady-state level of Rad51 increases in proteasomal mutants. Exponentially growing cells of the WT (WCG4a), *pre2-K108R* (YWH24), *pre3-T20A* (YUS1), *pup1-T30A* (YUS4), *ump1Δ* (YAS13), *rad5Δ* (YJM26), *rad6Δ* (YAZ10), *ufo1Δ* (YJD1), and *mms2Δ* (YJM56) strains [49,50], [25] were analyzed by WB to monitor the Rad51 level. The Rad51 signal was normalized to the proteins visualized by Ponceau S staining. The average fold increase versus the WT Rad51 level, which was set to 1.00, was then calculated (blue numbers below the blot). (d) Analysis of Rad51 ubiquitination in vivo by His-Ub affinity-isolation assay. WT (YJK1) and *pre2-K108R* (YJK2) strains bearing an empty vector YEp96 or a vector encoding His6-Ub and HA-Ub (control) from plasmids YEp96-Ubi-His (pUb-His) [33] and YEp112 (pUb-HA) [34], respectively, were grown in the presence of Cu^{2+} ions and collected. Ubiquitinated proteins were purified on Ni^{2+}-NTA sepharose from total extracts and analyzed by WB using anti-Rad51 antibodies. The position of Rad51 and poly-ubiquitinated Rad51 (Rad51-poly-Ub) are indicated on the right. Molecular mass markers are displayed on the left.

conditional mutants in the BY4741 background on the level of Rad51 (Fig. 2). The screen confirmed the dependence of Rad51 levels on proteasomal activities because a twofold increase of Rad51 was observed in all assayed *pre2* mutants and the *ump1Δ* strain, in agreement with our initial findings (Fig. 1 c). The screen further implicated a group of E2 and E3 enzymes that were likely to be involved in posttranslational Rad51 modifications because the lack of their proper function led to an increased Rad51 steady-state level. In particular, these included strains with mutations in Dia2 and Cdc4, the subunits of respective Skp1-Cullin1-F-box protein (SCF) Ub ligase complexes; RING finger proteins Rad5 and Rad18, as well as the SUMO-targeted Ub ligase (STUbL) Slx8 (Fig. 2 a). Similar phenotypes were seen in strains lacking: (i) Ub-conjugating enzymes Rad6, Mms2, and Ubc13 (cooperating with Rad18 or Rad5); (ii) subunits of the SCF complex Skp1, Cdc34, and Cdc53; (iii) or SUMO-ligases, such as Wss1 or a strain lacking both Siz1 and Nfi1/Siz2 SUMO-ligases (Fig. 2 a, b). Moreover, these results pointed out the importance of an anaphase-promoting complex (APC) for Rad51 stability because in *apc11–22* and *cdc23–1* strains, carrying mutations in APC subunits, the level of Rad51 was also elevated. Mutants that showed a significant decrease in the Rad51 level were strains lacking a functional Rsp5 protein (a NEDD4 family E3 Ub ligase) and the Prp19 protein whose U-box domain possesses E3 Ub ligase activity (Fig. 2 a).

3.3. SUMOylation contributes to Rad51 protein level regulation

As shown in Fig. 1 d, the Rad51 protein is poly-ubiquitinated in vivo. But among Ni^{2+}-NTA-bound protein fractions, the mono-ubiquitinated form of Rad51 was not visible. While studying the Rad51 WBs signals, we noticed another characteristic feature of this protein: it is represented by multiple bands. The weak band migrated just as expected for the Rad51 molecular mass (about 43 kDa), and the more pronounced forms migrated around 50 kDa (Fig. 3 a). For this mobility shift, the PTMs of Rad51 might be responsible. According to published data, several amino acid residues within the Rad51 sequence are subject to phosphorylation. Because the shift in Rad51 mobility visible on WBs can be estimated as

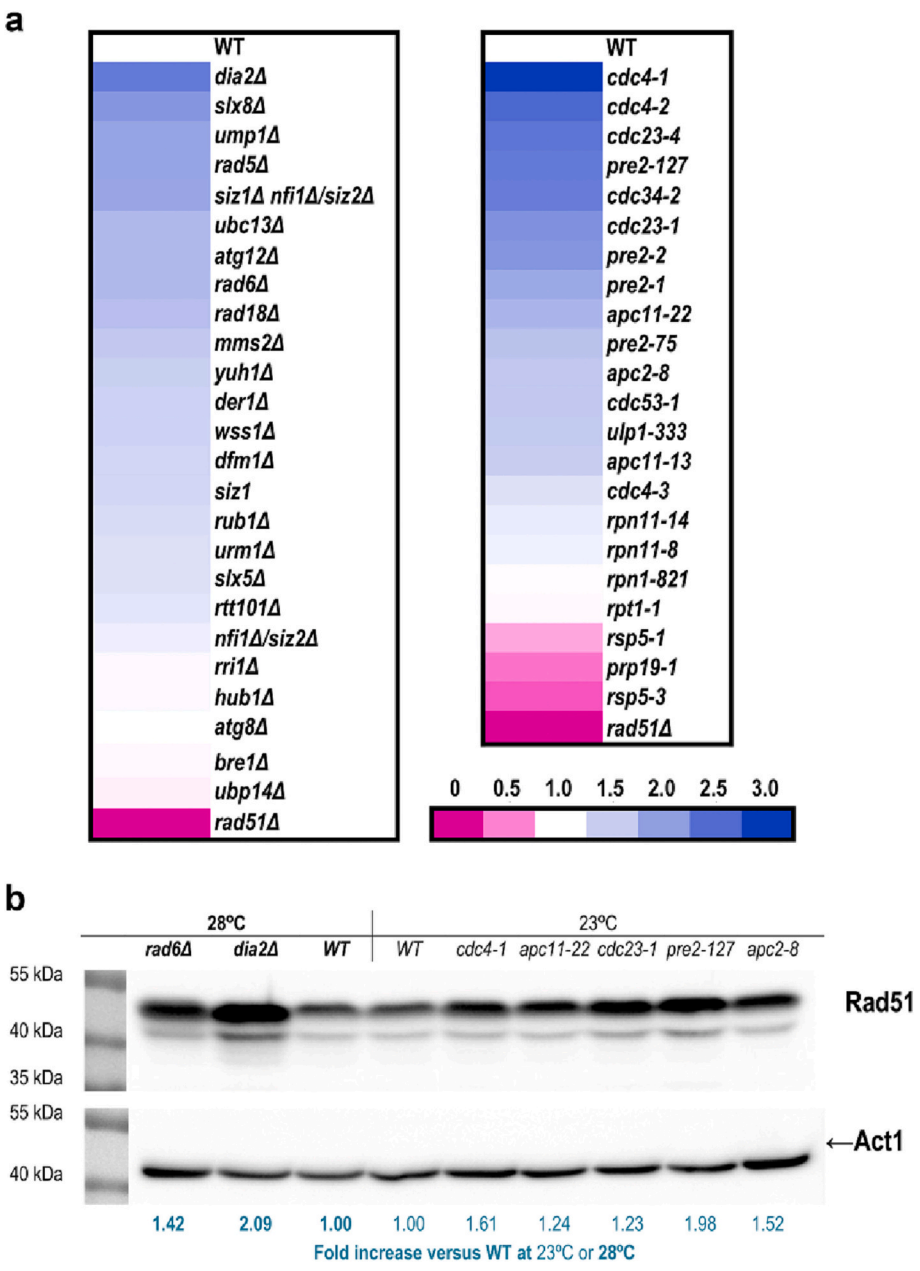

Fig. 2. Multiple E2 and E3 enzymes influence the Rad51 cellular level.
(a) Heat map showing the fold change of the Rad51 level in the indicated mutants relative to the level of this protein in the wild-type control. Strains in the BY4741 background, bearing defects in the genes encoding proteins involved in protein stability control via the Ub-dependent degradation pathway, were assayed by WB. Protein extracts were prepared from cells in the exponentially growing phase. From 2 to 6 independent biological replicates were made. The Rad51 signal was normalized to actin, a nonspecific band, or Ponceau S-stained proteins. The average fold change of Rad51 level relative to the WT cells is shown. The left and right panels show results obtained at 28 °C or 23 °C, respectively. (b) WB showing the dependence of Rad51 degradation on selected enzymes from the Ub-dependent degradation pathway. The differences in the fold-change numbers between the heat map and those given below the WB image, which were apparent for some strains, resulted from the variations between the biological replicates. Deletion strains *rad6Δ* and *dia2Δ* and the WT strain shown on the left were grown at 28 °C, and strains carrying point mutations in the essential genes *APC11*, *CDC23*, *CDC4*, and *PRE2* and the WT strain shown on the right were grown at 23 °C. Act1 is shown as a loading control. Blue numbers below the blot represent the fold increase of Rad51 level relative to the WT level, which was set to 1.00, calculated for the presented WB result. For the data obtained at 23 °C regular fonts were used, while for the data obtained at 28 °C bold fonts were used.

corresponding to a 7 to 8 kDa change in molecular mass of this protein, the probability that phosphorylation status is responsible seems unlikely. In contrast, the mass difference suggests a Ub-like modifier. To test such a hypothesis, we used a series of yeast mutants lacking genes encoding various Ub-like modifiers: Atg12 (involved in autophagy [52]), Hub1 (involved in budding and mating processes [53,54]), Rub1 (involved in neddylation of various substrates, e.g., cullins [55]), and Urm1 (involved in the glucose limitation response and oxidative stress response [56]). However, both the level of Rad51 and the position of the protein following SDS-PAGE were similar in all analyzed strains (Fig. 3 a).

Considering the absence of an affect with strains lacking these various Ub-like modifiers, we asked whether Rad51 is tagged with another such modifier, SUMO. In yeast, the SUMO protein is encoded by the *SMT3* gene. Because the *SMT3* gene is essential for cell viability we could not use a null strain. To overcome this limitation we first checked the Rad51 level in cells lacking two major SUMO E3 ligases, Siz1 and Nfi1/Siz2 [57,58]. The results showed no change in the Rad51 level in the *nfi1/siz2Δ* strain, a slight increase in the *siz1Δ* strain, and a significant increase in the double mutant *siz1Δ nfi1/siz2Δ* (Fig. 3 a). Additionally, the results drew our attention to the fact that one of the bands detected specifically by anti-Rad51 antibodies (the upper Rad51 band in Fig. 3 a) seemed to be a double in the samples derived from the double mutant *siz1Δ nfi1/siz2Δ*, and to some extent (with a much weaker lower band) also in *nfi1/siz2Δ and slx8Δ* samples. Therefore, we applied alternative separation conditions (acrylamide:bis-acrylamide [29:1], longer gels, and slow electrophoresis), which allowed for better separation of the two upper Rad51 bands. Subsequently, in the sample derived from the *siz1Δ nfi1/siz2Δ* strain, a clear band of slightly reduced intensity appeared below the Rad51 band migrating around 50 kDa (Fig. 3 b). Because unmodified Rad51 is predicted to migrate at approximately 43 kDa, this faster migrating Rad51 band likely corresponds to another form of post-translationally modified Rad51. The character of this modification is the subject of a separate study.

Because Rad51 accumulated not only in *siz1Δ nfi1/siz2Δ* cells but, according to our screen results (Fig. 2 a), also in *slx8Δ* cells lacking one

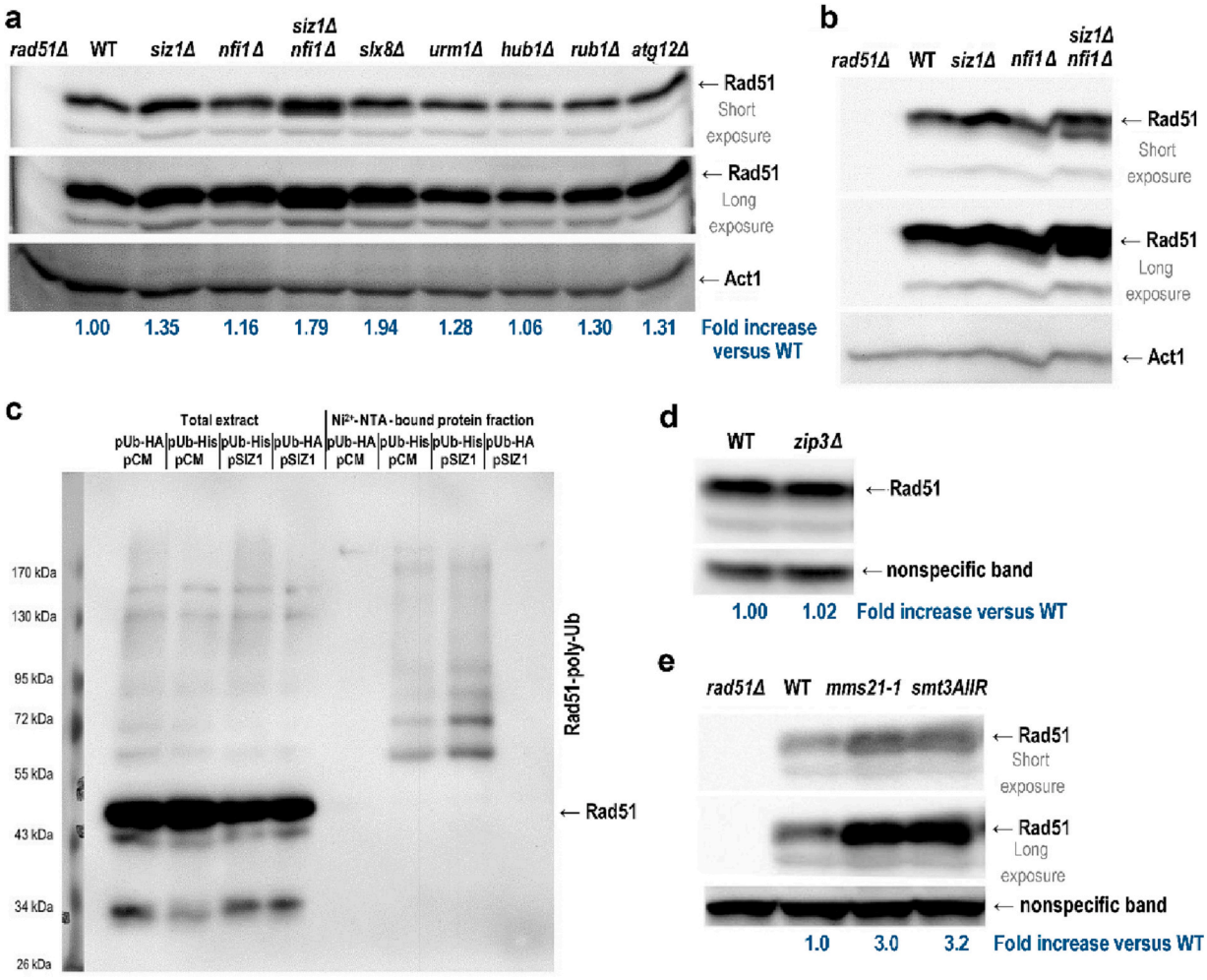

Fig. 3. SUMOylation promotes Rad51 destabilization.
(a) Rad51 accumulates in mutants lacking SUMO E3 ligases or STUbL complex subunit Slx8. Strains in the BY4741 background lacking the indicated genes were cultivated to an exponential growth phase, and then were subjected to WB analysis to detect Rad51. At least three independent biological replicates were made. The average fold increase versus the WT Rad51 level, which was set to 1.00, was then calculated (blue numbers below the blot). (b) A strong, additional Rad51-specific band was observed on the WB in the *siz1Δ nfi1/siz2Δ*-derived samples. (c) Analysis of Rad51 ubiquitination in vivo by His-Ub affinity-isolation assay. A WT (YJK1) strain bearing the plasmid YEp96-Ubi-His (pUb-His) [33] or YEp112 (pUb-HA) [34] and pCM188-SIZ1 (overexpressed Siz1) or the pCM188 empty vector, respectively, were grown in the presence of Cu^{2+} ions and collected. Ubiquitinated proteins were purified on a Ni^{2+}-NTA Sepharose column from total extracts and analyzed by WB using anti-Rad51 antibodies. Rad51 and poly-ubiquitinated Rad51 (Rad51-poly-Ub) are indicated on the right. Molecular mass markers were shown on the left. (d) A *zip3Δ* strain displays a Rad51 level similar to the WT strain. The WT and *zip3Δ* strain-derived samples were prepared and probed as in (a). (e) Rad51 accumulated in cells lacking Mms21 SUMO-ligase and in cells bearing an *smt3AllR*-encoding SUMO variant deprived of all its lysine residues, therefore, disabling chain structure formation. The WT, *mms21–1*, and *smt3AllR* strain-derived samples were prepared and probed as in (a). Act1 serves as a loading control in (a), (b) and (e), and a nonspecific band does so in (d). The average fold increase versus the WT Rad51 level, which was set to 1.00, was calculated from 3 to 5 biological repetitions (blue numbers below the blot).

of the yeasts STUbL enzymes, we asked if overproduction of SUMO E3 ligase would promote Rad51 ubiquitination. To answer this question, we overexpressed the SUMO E3 ligase Siz1, which simultaneously expressed a His-tagged Ub. In particular, we used a WT strain carrying two plasmids: a plasmid under the control of the inducible *CUP1* promoter encoding a His-tagged Ub variant [33] or HA-tagged Ub variant [34] (as a negative control), and a plasmid bearing the *SIZ1* gene under the tet_2O promoter or the empty vector pCM188 [31] as a control. Then, by using Ni^{2+}-NTA sepharose, we purified ubiquitinated proteins from these cells. WB analysis performed using anti-Rad51 antibodies detected enrichment in poly-ubiquitinated Rad51 forms among the Ni^{2+}-NTA-bound protein fraction in the sample derived from the strain overproducing Siz1 compared to the control (Fig. 3 c). In parallel, a decrease in Rad51 level was observed in the respective total extract sample. Together, these results led us to conclude that the Rad51 protein is poly-ubiquitinated in a Siz1- and SUMO-dependent fashion.

Several enzymes have SUMO E3 ligase activity in yeast. Besides the Siz1 and Nfi1/Siz2 SUMO E3 ligases mentioned above, a similar activity is displayed by other enzymes, such as Cst9/Zip3 or Mms21. Thus, we asked whether removing their activity would affect the Rad51 level. In the *zip3Δ* strain, we found no difference in the Rad51 level compared to the WT strain (Fig. 3 d), which could be expected because even though Zip3 activity is linked to DSB repair, it is mainly observed during meiosis [59,60]. However, in the *mms21–1* mutant [61,62] the Rad51 level was considerably increased (Fig. 3 e). This result provided a new link between SUMOylation and DSB repair, suggesting Rad51 to be a potential target of SUMOylation (e.g., by the Smc5-Smc6-Mms21 E3 complex during DSB repair, as predicted for yet unspecified DNA repair proteins engaged in brake-induced replication [63]).

Because various SUMO E3 ligases seem to keep the Rad51 level under control, facilitating or enabling Rad51 ubiquitination, we asked whether the presence of the SUMO chain is engaged in this process. Usage of an

smt3AllR [64] mutant, in which all lysine residues were replaced with arginine, preventing lysine-linked chain formation, enabled us to test this hypothesis. Indeed, the level of Rad51 in the *smt3AllR* mutant was significantly increased (Fig. 3 e).

The SUMO chain may recruit the STUbLs, which modify proteins to direct them for degradation. One such enzyme is the Slx5-Slx8 complex, and we asked whether this complex contributes to the Rad51 level limitation. We found that the Rad51 level was elevated in the *slx8Δ* mutant compared to the control (Fig. 3 a). All these results confirmed our hypothesis that SUMOylation is involved in Rad51 degradation.

3.4. Multiple enzymes regulate the ubiquitination of Rad51 in vivo

An increased Rad51 level was detected in strains lacking various E2 and E3 ligases (Fig. 2). Which of them is then responsible for the ubiquitination of Rad51? To address this issue, we used two opposite

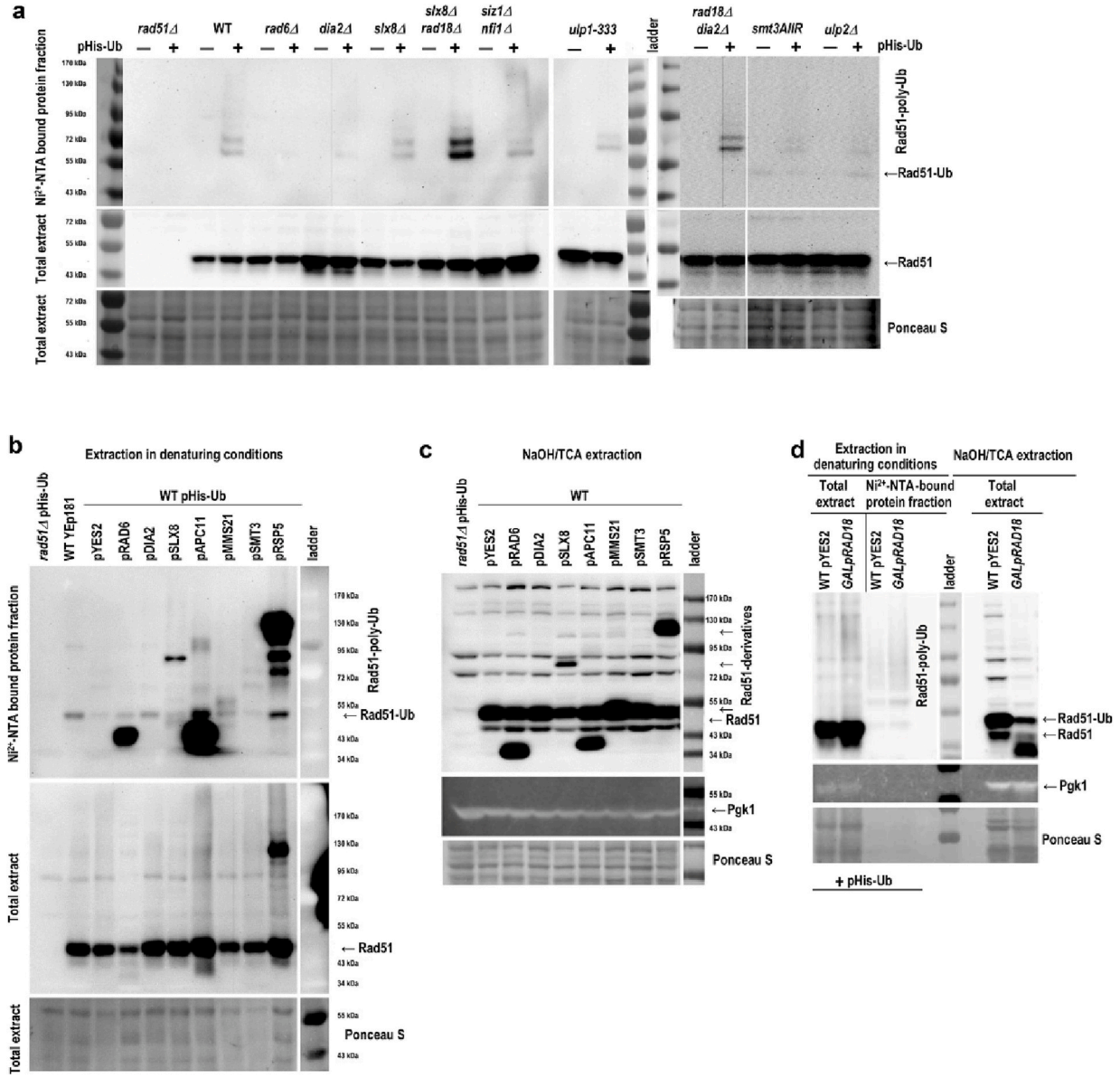

Fig. 4. Many enzymes affect the ubiquitination pattern of Rad51.
(a) Analysis of Rad51 ubiquitination by His-Ub affinity-isolation assay using BY4741 background strains with defects in the ubiquitination or SUMOylation pathways. Strains with YEp181-CUP1-His-Ubi [33] plasmid, grown to exponential phase, were induced with Cu^{2+} ions to produce His-tagged Ub. Ubiquitinated proteins were purified on a Ni^{2+}-NTA sepharose and analyzed by WB using anti-Rad51 antibodies. Rad51 and poly-ubiquitinated Rad51 (Rad51-Ub) bands are indicated on the right. Molecular mass markers are shown on the left. At the bottom, the blot containing total extracts stained with Ponceau S is shown. (b) Analysis of Rad51 ubiquitination by His-Ub affinity-isolation assay using strains overproducing the proteins involved in the ubiquitination and SUMOylation pathways. Strains in Y258 background bearing two plasmids, YEp181-CUP1-His-Ubi and pYES2 (control) or indicated plasmids from the MORF collection, and negative control (*rad51Δ* strains with the YEp181 and YEp181-CUP1-His-Ub plasmids) were grown to exponential phase. Production of His-tagged Ub and the indicated proteins was induced by Cu^{2+} ions and galactose, respectively. The ubiquitinated proteins purified on Ni^{2+}-NTA sepharose were analyzed by WB using anti-Rad51 antibodies. At the bottom, the result of Ponceau S staining of a blot containing total cell extracts is shown. (c) Analysis of Rad51 level in the strains overproducing the proteins involved in the ubiquitination and SUMOylation pathways. The same strains as in (b) but containing only MORF plasmid were grown to exponential phase, then induced 4-h on galactose. Collected cells underwent NaOH-TCA extraction, and samples were analyzed by WB to detect Rad51. At the bottom, the result of WB using anti-Pgk1 antibodies and a blot containing total extracts stained with Ponceau S are shown. (d) Analysis of Rad51 ubiquitination by His-Ub affinity-isolation assay using a *GAL1p-RAD18* (YAM27) and WT (BY4741) strain carrying plasmid YEp181-CUP1-His-Ub was performed as in (b).

approaches. First, we looked for E2 or E3 activities, whose absence resulted in the disappearance of Rad51 ubiquitinated forms from the cell. Second, we looked for enrichment of ubiquitinated forms of Rad51 when specific E2 or E3 enzymes were overproduced; we reasoned that increased activity in the conjugating and ligase enzymes would overwhelm the capacity of the degradative system, so that the ubiquitinated substrate would accumulate. In these experiments, we again took advantage of the His-tagged Ub system. After introducing a YEp181-CUP1-His-Ubi plasmid [36], expression from the *CUP1* promoter was induced with Cu^{2+} ions. Then, proteins were extracted from the cells, and the His-Ub-bound protein fraction was purified using Ni^{2+}-NTA sepharose and analyzed by WB using anti-Rad51 antibodies. Ubiquitinated Rad51 forms were absent in the samples prepared from *rad6Δ* and *dia2Δ* strains (Fig. 4 a), pointing to the importance of Rad6 (E2) and Dia2 (E3) for their formation.

Because we expected SUMO-targeted Rad51 ubiquitination, we included in our analysis strains defective in SUMO-chain formation (*smt3AllR*), lacking functional SUMO E3 ligases (*siz1Δ nfi1/siz2Δ*) or SUMO peptidases (*ulp1–333* and *ulp2Δ*). The ubiquitinated forms of Rad51 were absent or reduced substantially in the *smt3AllR* sample (Fig. 4 a). Thus, the inability to form SUMO chains or lack of appropriate enzymatic activity affects Rad51 ubiquitination.

Elevated Rad51 ubiquitination might be expected in the *ulp2Δ* sample due to the lack of SUMO peptidase activity. The virtual absence of Rad51 ubiquitination in this sample may be explained in several ways: (i) The absence of peptidase activity results in a reduction in the amount of free SUMO that is available for modifying Rad51, similar to the effect seen when free Ub pools are decreased by the deletion of *DOA4* [65]; (ii) SUMOylated Rad51 is a substrate for peptidases other than the Ulp2 isopeptidase; (iii) the accumulation of Rad51-SUMO forms in the *ulp2Δ* strain, stimulates a deubiquitinase, e.g., Wss1 [66], which removes Ub chains from that protein; (iv) SUMO influences Rad51 ubiquitination indirectly, via some Ulp2 substrates, e.g., Ub E3 ligase or SUMO E3 ligase, which in turn affect the Rad51 ubiquitination state. In the latter case, the higher rate of Rad51 ubiquitination in the strain overproducing Siz1 (Fig. 3 c) would be the result of activation of such an E3 ligase by SUMOylation in a Siz1-dependent fashion.

Among the analyzed strains lacking Ub E3 ligases, only the *dia2Δ* strain showed a reduction in the formation of Rad51 ubiquitinated forms (Fig. 4 a). Deleting the genes encoding individual Ub E3 ligases led to, at most, slight differences in the intensity of the higher molecular mass bands representing poly-ubiquitinated forms of Rad51 (Fig. 4 a). A similar effect was seen in the double deletion *dia2Δ rad18Δ* strain; however, when we eliminated the activity of two STUbLs, Slx8 and Rad18, we found enrichment in Rad51-Ub derivatives. There are alternative interpretations of this result. It is possible that abolishing one pathway marking Rad51 for degradation activates the backup one. Because a high level of Rad51 is toxic to the cells, the backup pathway that controls its level has evolved. It is worth mentioning here that the combination *slx8Δ dia2Δ* is synthetically lethal [67]. Thus, at least one of the Rad51 ubiquitination pathways has to work to preserve cell viability. The second interpretation considers the existence of Ub chains with different spatial geometry, e.g., linked via Lys63 or Lys48, etc. It is quite possible that the activities of individual E3 Ub ligases result in various types of Ub chains being added to Rad51 to determine its subsequent fate. These modifications do not necessarily guide the protein to the proteasome or vacuole for degradation; they could also act as a signal that activates recombinase function in response to stress. The elimination of E3 Ub ligases tagging Rad51 for degradation would reveal the Ub-tagging for other purposes by other specialized E3 ligases.

In the second line of experiments, we employed the strains from the MORF collection [38]. These strains carry plasmids expressing various yeast genes from the *GAL1p* promoter, which allows overproduction of selected proteins when strains grow in the presence of galactose. In our approach, we overexpressed genes of the selected E2 and E3 enzymes in the strains also producing His-Ub. This approach again allowed for purification of the His-Ub-tagged protein fraction on Ni^{2+}-NTA sepharose and further detection of ubiquitinated Rad51. The anti-Rad51 antibody recognizes mono-ubiquitinated Rad51 in all of the analyzed strains. The pattern of poly-ubiquitination of Rad51 varies between strains; however, the control sample (WT + empty vector pYES2) and Smt3 sample (WT + pSMT3) showed a similar pattern, but the intensity of bands was increased in the latter (Fig. 4 b). It seems that better access to SUMO promotes Rad51 ubiquitination. The most pronounced signals of ubiquitinated Rad51 were visible in the cells overproducing the Rsp5 Ub E3 ligase, suggesting that Rsp5 is responsible for Rad51 ubiquitination. This result, together with the reduced level of Rad51 in *rsp5–1* and *rsp5–3* mutants (Fig. 2 a), raises a question concerning the significance of Rsp5-dependent Rad51 ubiquitination, suggesting a role other than tagging the protein for degradation. It is worth noting that when only Rsp5 was overproduced, but not Ub, the level of the monomeric form of Rad51 (the band migrating at about 50 kDa) was lower compared to the situation when both proteins were overproduced (Fig. 4 c). Note that protein extraction in denaturing conditions from the cells overproducing Ub allows better preservation of the Rad51-Ub derivatives. In contrast, extraction using the NaOH-TCA method from the cells expressing endogenous Ub allows better visualization of protein turnover.

In the samples prepared from the cells overproducing the Slx8 subunit of the Slx5-Slx8 STUbL complex, the most intense band migrated at about 86 kDa (Fig. 4 b). However, other Rad51-Ub derivatives were also present in this sample including those visible in the sample prepared from cells expressing the gene encoding the Mms21 SUMO E3 ligase. In the samples prepared from cells expressing the Rad6 Ub-conjugating enzyme, the poly-ubiquitinated forms of Rad51 were hardly visible. Instead, a band migrating faster than the Rad51 monomeric band appeared, which indicated that poly-ubiquitinated Rad51 derivatives were short-lived in this strain leading to effective Rad51 degradation. Therefore, we concluded that Rad6 E2 activity contributes to Rad51-Ub tagging for degradation. Also, the overproduction of Apc11, the catalytic subunit of the APC complex (Ub E3 ligase), led to efficient Rad51 degradation (Fig. 4 c). However, the final digestion product migrated slower than that observed for cells overproducing Rad6. Moreover, the level of the monomeric form of Rad51 in the cells overproducing Apc11 did not drop down as was seen in the case of Rad6 overproduction (Fig. 4 b) but was higher than in the WT control. These results suggest the existence of different proteases that contribute to Rad51 digestion. Overall, control of the Rad51 level appears to involve multiple enzymes that may coordinate in a complex relationship.

The well-known partner of Rad6 (E2) is Rad18 (E3). To get an answer to the question of whether Rad51 ubiquitination depends also on Rad18 function, we prepared a yeast strain in which a *GAL1p::RAD18* fusion [30] replaced the genomic copy of *RAD18*; *RAD18* was expressed from the genome, but its expression was dependent on the presence of galactose in the media as a sole carbon source. We also introduced the YEp181-CUP1-His-Ub plasmid to this strain allowing us to take advantage of the different methods of protein extraction and differential level of production of the substrate for the ubiquitination reaction. After 4 h of growth on galactose and in Cu^{2+} ion-containing media, the ubiquitinated proteins were purified as above. Rad51 derivatives were visualized following SDS-PAGE separation with anti-Rad51 antibodies (Fig. 4 d). We found that Rad51 was ubiquitinated in a Rad18-dependent fashion (left panel). Moreover, this ubiquitination led to Rad51 degradation (right panel).

3.5. *Rad51 is SUMOylated*

Because the data described above pointed to the involvement of SUMOylation in the process of Rad51 level regulation, the question arose as to whether Rad51 is SUMOylated directly or whether the observed effects were the consequences of the SUMO-dependent regulation of enzymes influencing Rad51 stability. To answer this question, we performed the analysis of the Rad51 modification using protein

immunoprecipitation with anti-Rad51 antibodies and detection of SUMO and Ub derivatives among immunoprecipitated forms of Rad51. We found that Rad51 was SUMOylated in the samples purified from the strain overproducing the SUMO E3 ligase Mms21 and SUMO-ligase/SUMO-targeted metalloprotease Wss1 (Fig. 5, anti-Smt3). Different patterns of higher mass bands were detected with anti-Smt3 antibodies in the samples derived from strains overproducing Slx8 and Rsp5 Ub E3 ligases and Ulp1 protease, which cleaves specifically SUMO conjugates. In the latter sample, the lower mass form recognized by both anti-Rad51 antibody and anti-Smt3 antibody was also detected. The band of a similar mass was also seen in the sample derived from strain overproducing Apc11. In the sample derived from the strain overproducing Rad6, the band migrating even faster than that in the sample derived from the strain overproducing Apc11 was visible. Interestingly, using an anti-Ub antibody, we were able to show the poly-ubiquitination of Rad51. The poly-ubiquitinated forms of Rad51 were apparent in the sample derived from the strain overproducing Apc11 or Slx8; however, in the latter case, they migrated more slowly and were more pronounced (Fig. 5). This experiment showed that Rad51 undergoes two PTMs, ubiquitination, and SUMOylation. Furthermore, it seems that in some conditions both modifications could be introduced simultaneously.

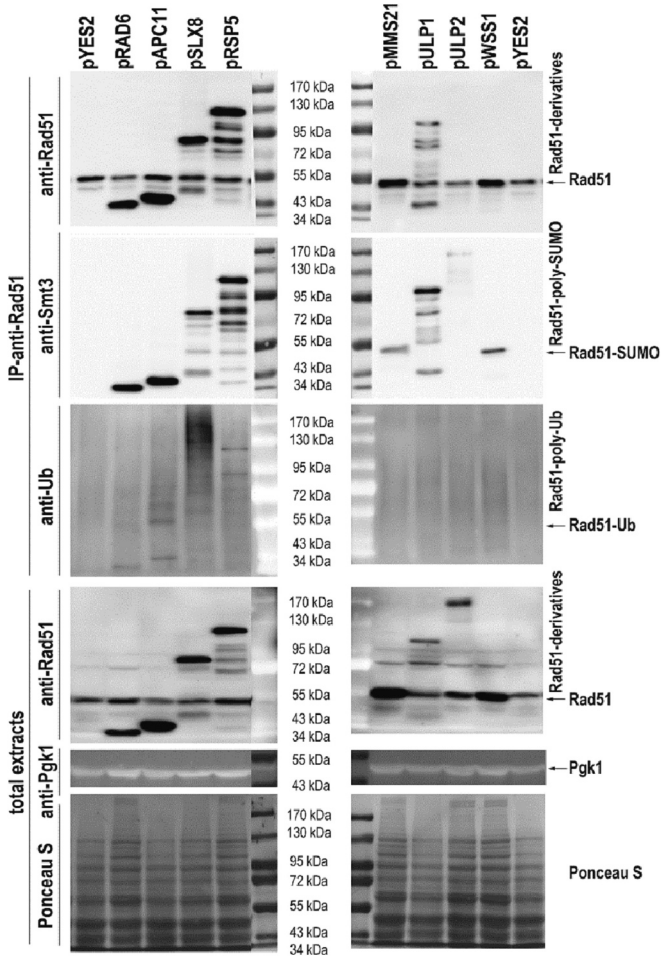

Fig. 5. Rad51 is SUMOylated in vivo.
Strains in the Y258 background, from the MORF collection, carrying the indicated expression plasmids or the pYES2 empty vector as a control, were cultivated to early exponential phase on SC-URA medium. Then the cells were harvested, washed, and allowed to grow for 4 h in a selective medium supplemented with 2 % galactose to induce expression from the *GAL1* promoter. Protein extracts were prepared and used for Rad51 immunoprecipitation as described in the Methods section. The immunoprecipitated proteins and total extracts were subject to SDS-PAGE, transfer, and WB with appropriate antibodies as indicated on the right side of the images. Because anti-Rad51 antibodies developed in rabbit were used for IP, we used the mouse anti-Ub antibodies and rabbit antibodies conjugated with HRP for Rad51 and Smt3 protein detection. On the total extracts blot, detection of proteins of interest was performed with rabbit anti-Rad51 antibody and mouse anti-Pgk1 antibody. At the bottom, the Ponceau S-stained blot with total extracts is shown.

Because SUMOylation of the Rad51 protein was shown in only one direct assay, namely in the Rad51 immunoprecipitation experiment, we decided to corroborate the presence of this modification with a second approach. Using the His-tagged Smt3 variant expressed from a plasmid [35] and the Ni^{2+}-NTA affinity assay, we looked for enrichment of SUMOylated forms of Rad51 when selected E3 enzymes were overproduced or missing. As shown in Fig. 6, SUMOylated Rad51 forms were hardly visible in the strains lacking Mms21, Slx8, and Rsp5, whereas pronounced additional bands of monoSUMOylated or poly-SUMOylated Rad51 appeared in the Ni^{2+}-NTA-bound protein fractions of yeast overproducing Mms21 or Slx8 and Rsp5, respectively. These data are in agreement with the results shown in Fig. 5 and support the conclusion that Rad51 is modified by SUMO, as well as illustrating the dependence of different SUMOylation patterns on these three E3 ligases.

3.6. Overexpression of E3 ligases affects Rad51 functioning in DNA repair, influencing cell morphology and viability

The biochemical studies described above demonstrated the presence of a wide selection of PTMs of Rad51 in yeast cells, but they did not reveal the biological role of these modifications. We attempted to get more information on this matter by applying fluorescence microscopy. It is known that Rad51 is recruited to the DNA damage site. It was also shown that such recruitment could be visualized as a fluorescence signal (repair foci) when a YFP-Rad51 protein fusion is introduced to the cell [37]; the more frequent the DNA damage, the more Rad51 foci are visible in the cell population. We used the YFP-Rad51 protein to monitor Rad51 foci formation in the cells overproducing selected E3 ligases. We chose Mms21 SUMO ligase that leads to mono-SUMOylation of Rad51, Slx8 STUbl that ubiquitinates SUMOylated Rad51, and Rsp5 ligase responsible for intense poly-SUMOylation/poly-ubiquitination of Rad51.

The results of the microscopy analysis showed that overexpression of E3 ligases, leading to different Rad51 SUMOylation and ubiquitination patterns, affected Rad51 ability to form repair foci. We observed a typical increase in the number of cells with Rad51 foci in all strains in the genotoxic stress condition. However, this increase was the highest in the strain overproducing Mms21 SUMO ligase. Also, in the control conditions, the cells with Rad51 foci appeared more frequently (twice more frequent) in this strain (Fig. 7 a, b). Moreover, the integrated density (i.e., the sum of the values of the pixels in the selected area) of Rad51 foci rose significantly in this strain compared to the control strain (Fig. 7 c). Therefore, mono-SUMOylation promotes Rad51 recruitment to DSBs and stimulates the increase of Rad51 foci size. The analysis also revealed a significant decrease in the number of cells with Rad51 foci in the strain overproducing Slx8 STUbL in the genotoxic stress conditions (Fig. 7 a-c). These data suggest that SUMO-targeted ubiquitination of Rad51 is required for Rad51 foci disassembly. A somewhat different effect was seen on the Rad51 foci formation with Rsp5 overproduction. In this case, the Rad51 foci seemed to form to a greater extent under genotoxic stress conditions than in the control strain, but their integrated density was slightly lower. This result suggests that the decoration of Rad51 with poly-SUMO and/or poly-Ub chains stimulates Rad51 foci formation but permits their reorganization/rearrangement and adjustment of their size.

To find out how Rad51 PTMs influence cells' susceptibility to genotoxic stress, we performed a sensitivity drop assay. In this set of experiments, we asked how the overproduction of E3 ligases affects cells' sensitivity to the alkylation agent MMS, replication stress induced with HU, and DSB stress provoked by zeocin. In addition, we asked if the Rad51 presence in the cells influenced the observed phenotypes. It was

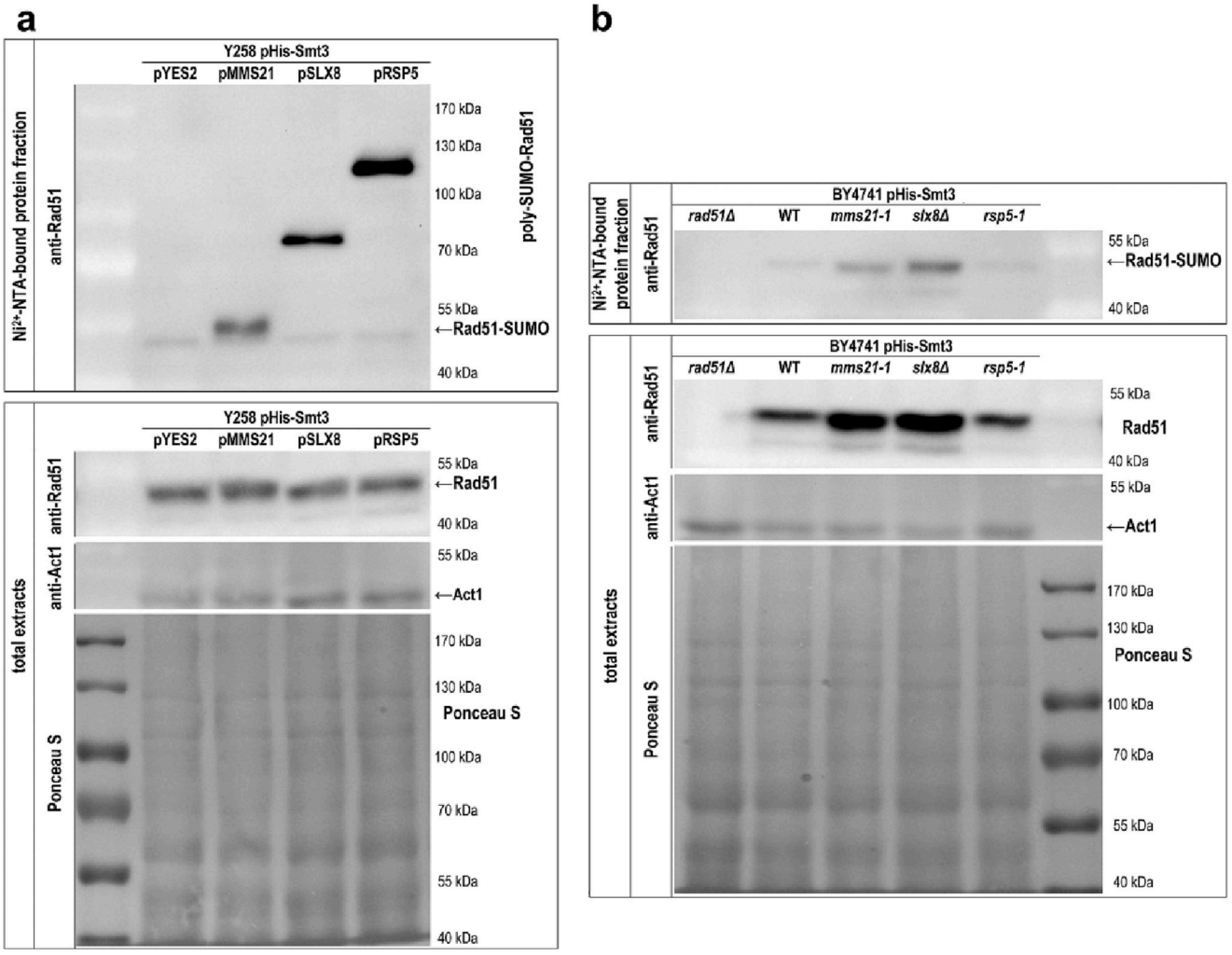

Fig. 6. Rad51 SUMOylation depends on Mms21, Slx8, and Rsp5.
(a) Strains from the MORF collection, in the Y258 background, carrying the indicated expression plasmids or the pYES2 empty vector as a control, were transformed with YEp181-CUP1-His-Smt3 [35] and were cultivated to early exponential phase on SC-URA-LEU medium. Then the cells were harvested, washed, and allowed to grow for 4 h in a selective medium supplemented with 2 % galactose and 100 μM $CuSO_4$ to induce expression from the *GAL1* and *CUP1* promoters, respectively. Protein extracts were prepared and used in a Ni^{2+}-NTA affinity assay as described in the Materials and methods section. The Ni^{2+}-NTA-bound proteins and total extracts were subject to SDS-PAGE, transfer, and WB with appropriate antibodies, as indicated in the images. To avoid possible false signals, we used anti-Rad51 antibodies conjugated with HRP. On the total extracts blot, the detection of proteins of interest was performed with rabbit anti-Rad51-HRP antibody and mouse anti-Act1 antibody. At the bottom, the Ponceau S-stained blot with total extracts is shown. (b) Strains in the BY4741 background, carrying the indicated mutations and YEp181-CUP1-His-Smt3 plasmid, were cultivated in SC-LEU medium. The induction of the *CUP1* promoter was obtained by 4-h incubation with the addition of $CuSO_4$ to the medium to a final concentration of 100 μM. Protein extraction, sample preparation, and WB analysis were performed as in (a).

clear that the episomally expressed *RAD51* complemented the *rad51Δ* cells' hypersensitivity to genotoxic compounds (Fig. 7 d). Interestingly, additional expression of genes encoding analyzed ligases influenced the ability of cells to grow in the tested conditions but in different ways. When Slx8 STUbL was overproduced, Rad51 complemented the *rad51Δ* sensitivity to genotoxic stress as well as in the control strain, or even better in the case of MMS stress. Overproduction of Mms21 led to a worse complementation potential of Rad51. It looked like the mono-SUMOylated Rad51 could not fully complement the *rad51Δ* strain hypersensitivity to genotoxic stresses. When Rsp5 was overproduced, the presence of Rad51 appeared not to have an impact on *rad51Δ* strain sensitivity.

During the microscopy analysis, we noticed morphological changes of the analyzed cells in certain conditions. For example, the overproduction of Rsp5 frequently led to cell elongation. To find out whether the atypical phenotype is caused by Rsp5 influence on actin cytoskeleton dynamics [68], filamentous growth provoked by glucose depletion (required for *GAL1p* induction) [69], or rather aberrant division, we performed two complementary assays, in which we analyzed fluorescently labeled yeast cells. In the first attempt, we used fluorescence microscopy of DAPI-stained cells overproducing E3 ligases in the *rad51Δ* background. The *rad51Δ* cells overproducing Rsp5 were polyploid cells with several nuclei distributed along the elongated cells, suggesting the enlargement of the cells was due to mitotic division problems leading to polyploidy (Fig. 7 e). The introduction of a pRAD51 plasmid to the same strain suppressed these morphological changes. The opposite effect was seen in the *rad51Δ* cells overproducing the Slx8 STUbL. Thus, cells changed their morphology when Rad51 was present; however, the morphology of the affected strains was slightly different. In the second attempt, we asked if the DNA content of the strains overproducing selected E3 ligases would change depending on whether Rad51 is present in or not and if this change correlated with the cell size changes. Fig. 7 f summarizes the results of flow cytometry analysis of propidium iodide-stained cell populations. First, the higher the DNA content, the bigger the cell size. Second, the phenotypic changes seen in the microscopy examination for the cells overproducing Rsp5 or Mms21 were

confirmed by flow cytometry analysis. Thus, they were frequent in the population. Also, flow cytometry suggested cell cycle anomalies in the analyzed strains. Overproduction of Mms21 in the *rad51Δ* strain caused the overrepresentation of S phase cells in the asynchronous population. In the same strain producing Rad51, cells could finish the S phase but not mitosis, resulting in polyploid cells. Overproduction of Slx8 in the *rad51Δ* strain shifted the cell cycle balance in favor of the G_1 phase, mainly when Rad51 was expressed. Therefore, E3 ligase-dependent modifications of Rad51 affected cell size and morphology by influencing the cell cycle in a Rad51-dependent manner.

4. Discussion

Rad51 recombinase plays such a crucial role in the cell that its level and activity have to be tightly regulated. Both depletion of Rad51 and its high level leads to a series of defects in the DNA damage response

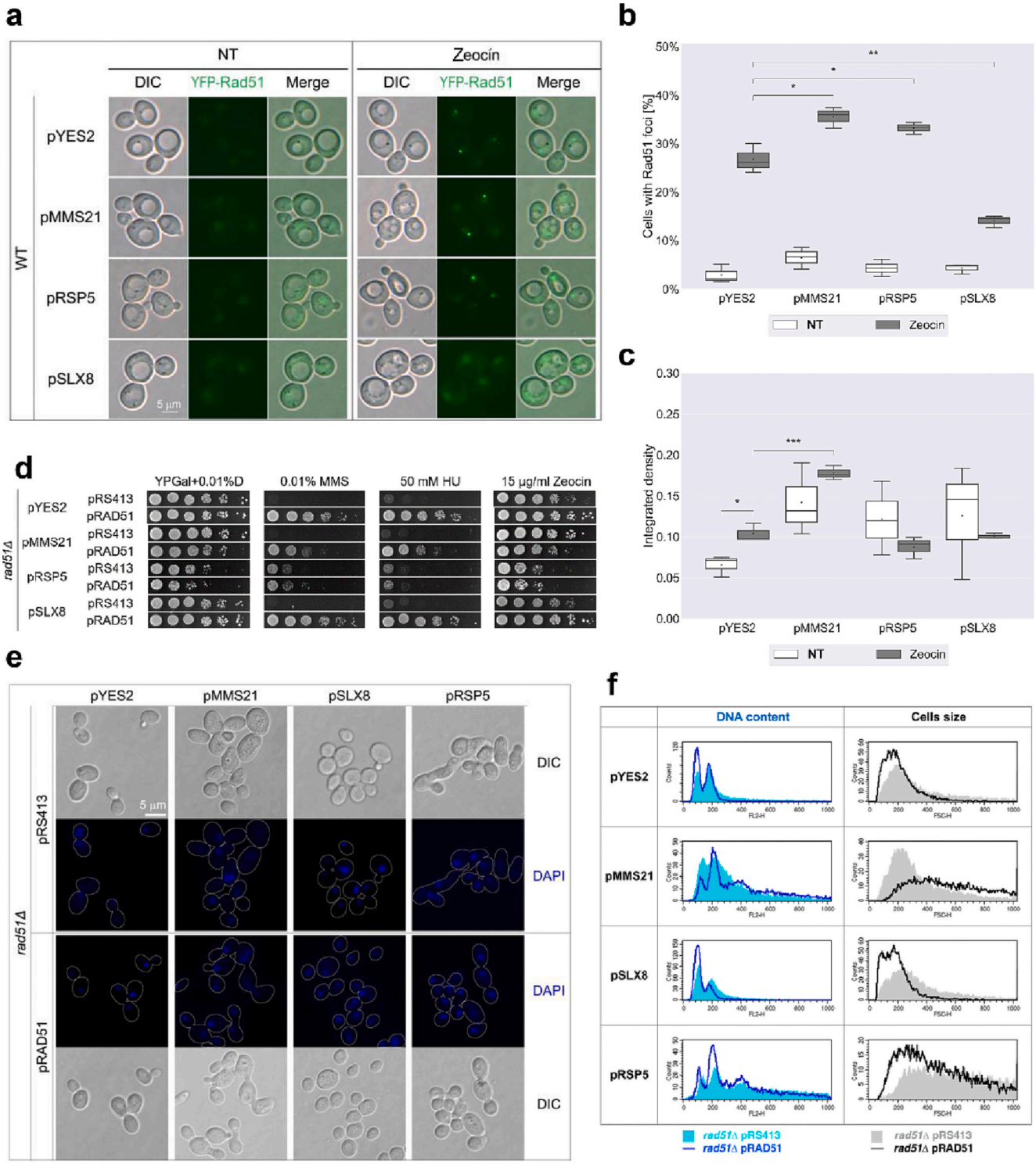

(caption on next page)

Fig. 7. Rad51-dependent phenotypic changes that accompany overproduction of E3 ligases in yeast cells.
(a-c) Overexpression of E3 ligases affects Rad51 foci number and intensity. Strain W4121—20D (*YFP-RAD51*) with plasmids pYES2, pMMS21, pSLX8, and pRSP5 were cultivated on galactose with and without zeocin and analyzed using microscope. (a) Sample photos are shown. The magnification is the same for all images and the scale bar (5 μm) corresponds to all panels. (b) Graph showing the number of cells with Rad51-YFP foci in the analyzed strains and conditions. Three biological repeats were analyzed, with a minimum number of 200 cells for each data point. Boxes represent the quartiles of data. Horizontal lines in the boxes represent the median values. The dot represents the mean value. Whiskers represent standard deviation. Data distributions were determined through a Shapiro-Wilk test. Statistical hypothesis testing were conducted by *t*-test for independent means. *p-val < 0.05; **p-val < 0.01. For clarity, the statistically significant difference (p-val < 0.0001) in the Rad51 foci number between non-treated and zeocin-treated cells was omitted from the graph. (c) Rad51 foci intensity displayed by integrated density. Integrated densities were calculated for each individual foci in the cells, which in this case is described as the sum of the values of the pixels in the area of foci. Analyzed foci were arranged based on the corresponding biological repeat. *p-val < 0.05; ***p-val < 0.001. The other descriptions as in (b). (d) Overexpression of E3 ligases affected the cells' sensitivity to various genotoxic agents. Strain BY4741 *rad51Δ* (WT) carrying the same plasmids as in (a) but also plasmid pRAD51 or pRS413 were cultivated in the selection medium with glucose, then the carbon source in the medium was changed to galactose, and cells were tested for their sensitivity to different genotoxic compounds. The strains growth after two days of incubation at 28 °C is shown. (e) The morphological changes in analyzed strains are E3 ligase- and Rad51-dependent. The same strains grown to the exponential phase in the conditions as in (d) were stained with DAPI and analyzed using fluorescence microscopy. The representative photos are shown. The magnification is the same for all images and the scale bar (5 μm) corresponds to all panels. (f) The DNA content and cell size depends on the presence of E3 ligases and Rad51. Flow cytometry analysis was performed for the propidium iodide-stained cells of the strains as in (d). The representative histograms for each strain are shown.

[9,22,70,71]. In more complex eukaryotes, Rad51 deficiency results in cell death due to DSBs accumulation [72]. In humans, several Rad51 orthologs (including RAD51, BRCA1, and BRCA2) contribute to genome stability and frequently predispose to cancer when mutated [73]. Also a high level of RAD51 is a bad prognostic in various cancers [74,75]. During DNA damage repair Rad51 acts through formation of a filament on single-stranded DNA. Forming the nucleofilament is essential for the initial steps of HR, including DNA sequence homology search, recruitment of DNA repair proteins and protein complexes involved in chromatin remodeling, which together enable repair of DNA damage such as DNA breaks or cross-links [76].

In our work, we aimed to uncover the regulation of the cellular Rad51 level and identify the factors contributing to this regulation. The level of Rad51 protein was increased in *pre2–1*, *pre3–1*, *pup3–1*, and *ump1Δ* mutants, suggesting proteasomal degradation of this protein. In agreement with this result, we showed Rad51 poly-ubiquitination. We found that the Rad51 level is actively regulated by proteasomal degradation, and its half-life is increased after genotoxic stresses (Fig. 1). Similar observation was made by Woo and colleagues when they used the proteasome inhibitor MG132 to determine if Rad51 is degraded by the proteasome during the DNA damage response [77]. We also identified several Ub-conjugating enzymes (E2) and Ub ligases (E3) affecting the Rad51 cellular level. The level of Rad51 is elevated in *rad6Δ* and *ubc13Δ*, as well as in *rad18Δ* and *rad5Δ* strains (lacking E2 and E3 enzymes, respectively). Besides RING finger-type E3 Ub ligases (Rad5 and Rad18), also F-box proteins, Dia2 and Cdc4, subunits of SCF^{Dia2} and SCF^{Cdc4} Ub ligase complexes, respectively, seems to regulate the Rad51 level because, in *dia2Δ* and *cdc4–1* mutant cells, the level of Rad51 was doubled compared to the control strain level (Fig. 2). Additionally, we found that the STUbL, the Slx5-Slx8 complex, contributed to Ub-dependent Rad51 regulation. In accordance with this result, we found an increased level of Rad51 protein in an *mms21–1* mutant, as well as in a *siz1Δ nfi1/siz2Δ* strain lacking two other yeast SUMO ligases. Also, the poly-ubiquitinated forms of Rad51 were enriched in cells overproducing the SUMO E3 ligase Siz1 or Smt3 (a yeast SUMO variant). Thus, Rad51 degradation is Ub and SUMO dependent (Figs. 3, 4, 5).

The similarities of DNA damage response pathways between different species, accumulating protein data in protein databases and bioinformatics tools predicting modification sites, suggest that the budding yeast Rad51 protein, like its homologs from human, mouse, nematode or radish, should be SUMOylated [78]. There are also at least two examples showing the Ub modification of yeast Rad51 homologs. In human cells, RFWD3-dependent ubiquitination of RAD51 leads to its proteasomal degradation [79]. In *Schizosaccharomyces pombe* Rad51 ubiquitination depends on Rrp1 [80]. Thus, we could expect the direct modification of Rad51 also in *S. cerevisiae*.

By showing the influence of E3 Ub and SUMO ligase overproduction on the basal level of Rad51 and the appearance of higher molecular mass Rad51 forms in the cell, we indicated which of them are involved in regulating the Rad51 level. But we also showed that at least some of these enzymes modify Rad51 with PTMs. In particular, we established the fact that Rad51 is SUMOylated and ubiquitinated in vivo. Thus, we found that another DNA-binding protein that plays an important role in tunneling the DNA damage response pathways is regulated via SUMOylation. A well-known example of the role of PTMs in the repair pathways choice in response to replication stress is the PCNA complex, whose modification with SUMO/Ub determines if the replication block will be overcome by the respective DNA polymerase in the trans-lesion synthesis pathway or with recombination usage in the DNA damage avoidance pathway [81,82].

The SUMOylation of Rad51 depends on Mms21, and Wss1 SUMO E3 ligases (Figs. 5, 6). The ubiquitination of Rad51 depends on Rad6-Rad18, Dia2, Apc11, Slx8, and Rsp5 Ub E3 ligases (Figs. 4, 5). However, the modification network seems to work in a complex way with respect to Rad51 stability. Modification with Ub or SUMO appears to be bifunctional. In some circumstances it leads to Rad51 degradation, whereas in others it stabilizes the protein. In addition, some of the observed effects seem to be indirect, e.g., the role of Siz1 E3 SUMO ligase in Rad51 stability. On the one hand, we showed a decreased level of Rad51 monomers and increased poly-ubiquitination of Rad51 when Siz1 was overproduced (Fig. 3 c). On the other hand, we did not see the SUMOylated form of Rad51 among immunoprecipitated Rad51 derivatives, nor among a SUMOylated protein fraction enriched on the Ni^{2+}-NTA sepharose from the cells overproducing both His-tagged Smt3 and Siz1 (data not shown). We postulate that Siz1 SUMOylates the proteins that contribute to Rad51 stability. At least two such proteins could be implicated. Rsp5 is subject to Siz1-dependent SUMOylation, which results in its reduced Ub ligase activity [83]. Because Rsp5 stabilizes Rad51, the activity of Siz1 will stimulate Rad51 degradation. The other Siz1 substrate is Pol30, the yeast proliferating cell nuclear antigen (PCNA), the ring-shaped trimeric complex that encircles DNA and functions as a sliding clamp and processivity factor for replicative DNA polymerases [83–85]. SUMOylated PCNA recruits Srs2 and Rad18, triggering Srs2 activity of Rad51 translocase and Rad18 activity of Ub ligase, which both act in an anti-recombinogenic manner and likely influence further Rad51 cellular fate [30], [86–89]. We do not know what happens to Rad51 protein stripped-off from DNA by the Srs2 helicase/translocase, but we showed that Rad51 might be SUMOylated and that one of the STUbLs involved in its poly-ubiquitination is Rad18 (Fig. 4).

The monomeric form of Rad51 detected on WBs with the specific anti-Rad51 antibody migrates as two or three bands (dependent on the strain background), with a molecular mass of about 43 kDa (the theoretical mass of Rad51), 50 kDa (likely a mono-ubiquitinated Rad51), and 52 kDa (likely a mono-SUMOylated Rad51). Indeed, the mono-ubiquitinated Rad51 was detected among the Ni^{2+}-NTA-bound protein

fraction of His-Ub-tagged proteins in almost all analyzed strains from the MORF collection overproducing E3 Ub ligases. The most pronounced signal was visible in the samples derived from strains overproducing Apc11, a catalytic subunit of the APC complex (i.e., a Ub ligase, whose activity enables metaphase/anaphase transition during mitosis via tagging with Ub the anaphase inhibitors leading to their degradation) and Rsp5, a NEDD4 family E3 Ub ligase (involved among others in such processes as MVB sorting, endocytosis or the heat shock response) (Fig. 4 b). Likely due to distinct biological processes in which these two ligases are involved, the pattern of other Rad51 bands accompanying the mono-ubiquitinated Rad51 monomer is totally different. When Apc11 was overproduced, we also saw the poly-ubiquitinated forms of Rad51 (Fig. 4 b, 5). Still, the most prominent Rad51 band observed for this sample migrated as 43 kDa, i.e., exactly as expected for a non-modified Rad51 protein. Only a band of that mass was observed among proteins modified with the His-tagged variant of Ub. Thus, this species probably represents a degradation product of Rad51, shortened by about 9 kDa. When Rsp5 was overproduced, we saw additional bands of Rad51 migrating slower than mono-ubiquitinated Rad51. These bands may reflect poly-ubiquitinated forms of Rad51; however, some of them had a mass which is a duplication or triplication of the Rad51 mass. Thus, it is also possible that the bands reflect oligomers of Rad51 (supposing formation of covalent bonds between Rad51 molecules). In such a case, the process of Rad51 oligomerization would be stimulated by ubiquitination with the Ub E3 ligase Rsp5 (Fig. 4 b, Fig. 5). Interestingly, the upper Rad51 bands appeared not only when we detected ubiquitinated Rad51 derivatives but also when we detected SUMOylated Rad51 forms (Fig. 5). However, the pattern of SUMOylated forms only partially overlaps with the pattern of ubiquitinated forms. The results led us to conclude that part of the cellular Rad51 pool might be modified with SUMO and Ub or might possess mixed SUMO and Ub chains. Also, the availability of substrates for protein modification and the local concentrations of E3 ligases may determine the future fate of the protein.

Acquired data pointed to three Ub E3 ligases, whose activities result in the poly-ubiquitination and subsequent degradation of Rad51. Besides Apc11, we confirmed Rad18-dependent and Slx8-dependent-poly-ubiquitination of Rad51 (Fig. 4 b, 4 d, 5). Interestingly, the Rad51 degradation product detected in the samples overproducing Rad18 migrated faster than that seen in the samples overproducing Apc11. Moreover, in the samples overproducing Rad6, a Rad51 degradation product appears, which had the same size as the one detected in the sample with Rad18 overproduction. The E2 Ub-conjugating enzyme Rad6 cooperates with Rad18 to mono-ubiquitinate PCNA at Lys164 in response to DNA damage stress [81]. The difference in the size between Rad51 degradation products appearing in the diverse conditions suggests the involvement of distinct peptidases in the degradation of this protein. Why do the additional peptidases have to be involved? First, because a high level of Rad51 is harmful for the cells, the backup systems evolved that allow the elimination of excess Rad51 when this is required. Second, the Rad51 nucleofilament might be a difficult target for degradation. Possibly, it has to be disassembled piece by piece before being sent to the proteasome for final digestion. The specialized peptidases might play an important role in this process. We presume that various enzymes tagging Rad51 protein for degradation and various peptidases could be involved in its degradation at different cell cycle phases. For example, the APC complex would be necessary for Rad51 degradation during mitosis, likely during the metaphase/anaphase transition, while the Rad6-Rad18 complex would play a similar role during the S phase of the cell cycle especially during DNA damage stress. Also, PTMs of Rad51 might have a crucial role in cell physiology, e.g., enabling Rad51 recruitment to the DNA damage site, formation and reorganization of the Rad51 filament during the DNA repair process, and its final decomposition. Indeed, the phenotypic changes we documented for the cells overproducing various E3 ligases favor this hypothesis.

Among Ub E3 ligases that contribute to Rad51 poly-ubiquitination, there are two enzymes belonging to the STUbLs, Rad18 and Slx8 [30,90]. However, the patterns of Rad51-derivatives purified from cells overproducing Rad18 or Slx8 were different. While overproduction of Rad18 caused an increased poly-ubiquitination of Rad51 accompanied by the appearance of the primary/major degradation product, overproduction of Slx8 led to increased poly-ubiquitination of Rad51 and the appearance of an additional protein band of about 80 kDa (Fig. 4 b, Fig. 5, Fig. 6). Puzzling is the fact that an 80-kDa protein band was visible in samples from cells overproducing Slx8 both after Ni^{2+}-NTA sepharose enrichment of ubiquitinated and SUMOylated proteins, but also after anti-Rad51 immunoprecipitation. This band was detected both with anti-Smt3 and anti-Rad51 antibodies. Thus, this protein likely possesses both Ub and SUMO modifications. Notably, the SUMO signal was more pronounced. Interestingly, poly-ubiquitinated forms of Rad51 released from the cells overproducing Slx8 had a mass over 80 kDa. We did not detect the degradation product of Rad51 in these cells; however, the level of Rad51 monomers was decreased in total extracts from the cells overproducing Slx8, at least when His-tagged Ub was not overproduced in parallel. A protein of similar mass was also observed when Rsp5 ligase was overproduced; but in this case it was accompanied by additional Rad51 derivatives of higher mass. We wonder, what exactly is the derivative of Rad51 that has a mass higher than 80 kDa? This species could be the Rad51 monomer modified with a SUMO/Ub chain or the Rad51 dimer, the formation of which was stimulated by PTM. We cannot exclude any of these possibilities yet.

This puzzle could be resolved by experiments made with the usage of *RAD51* alleles containing point mutations that prevent modifications. The problem is that there are 17 lysine and 8 cysteine residues in the Rad51 protein, which can be modified by Ub or SUMO. Three published datasets from proteomic approaches indicated the Rad51 amino acid residues modified with Ub or SUMO. A proteomic screen for meiotic SUMO targets revealed, among the others, the Lys122 residue in Rad51 [91]. In two other screens, the Lys131 residue was indicated as a ubiquitination site [92,93]. Moreover, Back and colleagues showed that K63-linked poly-Ub chains might modify Lys131 in response to oxidative stress [93]. Among various types of Ub chains, which might be conjugated to the protein substrates, the K63-linked poly-Ub chain is thought not to be involved in protein degradation by the proteasome but mainly used as signals in DNA repair, trafficking, and autophagy [94].

SUMOylation and ubiquitination seem to regulate various processes crucial for genome maintenance, e.g., replication, DNA repair, and chromosome segregation. Depending on the type of modification added to PCNA, different DNA repair pathways are used, so SUMO and Ub act as molecular switches between the inhibition of HR (PCNA-SUMO), trans-lesion synthesis (PCNA-Ub), and DNA damage avoidance (PCNA-poly-Ub) [85,95]. Also, the length and geometry of the Ub-chain does matter, altering the effect on the DNA damage bypass by poly-ubiquitinated PCNA [96]. Repairing replication forks stalled due to harmful DNA secondary structures (e.g., stem-loops) or DNA lesions (e.g., persistent DSBs) depends on the SUMOylation/ubiquitination pattern of proteins engaged in the repair, as well. The Mms21-dependent SUMOylation of DNA repair proteins associated with a stalled replication fork (e.g., RPA complex, Rad52, and Rad59) mediates their relocation to the nuclear periphery for repair. However, two destinations are possible. Mono-SUMOylated DNA repair proteins would be targeted to the Mps3 complex to be repaired with HR, while DNA repair proteins poly-SUMOylated in the Slx5-dependent manner would be targeted to the nuclear pore complexes to constrain recombination at stalled or collapsed forks until it is required for fork restart. The recruitment of the Slx8 Ub STUbL to the nuclear pore complex leads to poly-ubiquitination of DNA repair proteins and likely their degradation, which favors repair via error-prone pathways, such as ectopic break-induced replication and imprecise end-joining [63,97].

We do not know yet how exactly SUMOylation and ubiquitination influence the activity of Rad51 at the molecular level. However, the data we presented here (Fig. 7), indicated that they certainly affect its activity in the DNA repair process and protection against genotoxic stress. We

showed the mono-SUMOylation of Rad51 results in its enhanced recruitment to DNA, which does not necessarily translate into increased cell viability during genotoxic stress. On the contrary, an increased pool of mono-SUMO-Rad51 led to a drop-down in cell viability upon genotoxic stress, no matter what kind of stress was applied (alkylation stress, replication stress, or DSB stress). We concluded that the mono-SUMOylation of Rad51 not only simplifies the recruitment of this protein to DNA but also prevents Rad51 repair foci disassembling, leading to their excessive increase and overstabilization, which became toxic to the cells. The cell morphological changes and nucleus aberrations accompanying the increased Rad51 mono-SUMOylation level in the strain overproducing Mms21 SUMO ligase that we observed, likely caused by cell division problems (Fig. 7 e), were in line with this hypothesis. Especially since SUMO ligase activity of Mms21 is required in mitosis, response to genotoxic stress, and various aspects of genome maintenance, e.g., preventing telomere clustering, accumulation of DNA lesions, and toxic X-structures in DNA [61,98]. Also, the effective complementation with pRAD51 plasmid of hypersensitivity of the *rad51Δ* strain overproducing the Slx8 Ub ligase supports this hypothesis. From a physiological point of view, avoiding persistent Rad51 foci is of greater importance than their high number. Again, there is additional support for this conclusion from already published data. The repair of topoisomerase DNA cross-links by engaging Ub-mediated proteasomal degradation in a SUMO-dependent fashion is conserved in yeast and human. This process requires modification of trapped topoisomerase by SUMO ligase, followed by its ubiquitination, which drives at least partial proteasomal degradation of topoisomerase. This degradation opens access for the removal of the remaining topoisomerase from DNA via cleavage by tyrosyl-DNA phosphodiesterase I (Tdp1) or activity of one of the structural DNA endonucleases, leading to the final release of neat DNA ends. The initial part of this process relies on Siz1 or Mms21 SUMO ligase and Slx5-Slx8 STUbL in *S. cerevisiae* (in humans, PIAS4, and RNF4, respectively) [99,100]. Interestingly, also in human cells, the recruitment of RAD51 to chromatin and its interaction with BRCA2, which are crucial for HR efficiency in DSB repair, are promoted by TOPORS-dependent RAD51 SUMOylation [101]. The involvement of Rad51 ubiquitination in the repair foci decomposition was shown for another Rad51 homolog, the *S. pombe* Rad51 [80]. However, in this case, the modification depends on the bi-functional enzyme DEAD-like helicase/RING finger E3 Ub ligase, which seems to use both activities to remove Rad51 filaments from DNA.

Overproduction of Rsp5 in the *rad51Δ* strain led to both sensitivity to genotoxic stress and aberrant divisions (Fig. 7). It is worth mentioning here that overproduction of Rsp5 differentially affected the *rad51Δ* strain sensitivity to MMS and zeocin relative to the control strain, sensitizing cells to DSB stress but desensitizing them to MMS. This result suggested a specialized response to the particular genotoxic compounds in the analyzed genetic background. However, we did not see any Rad51-dependent effect on cell viability in these conditions, even though the Rad51 foci appeared more frequently during genotoxic stress when Rsp5 was overproduced, and the presence of Rad51 rescued the morphological abnormalities observed in this strain, including division abnormalities. We think an excess of Rsp5 is toxic to the cells in genotoxic-stress conditions due to the Rsp5 substrates ither than Rad51, which are more critical for cell viability in such situations. Several known substrates of Rsp5 Ub ligase might be taken for consideration because Rsp5 controls the degradation of RPA subunit Rfa1 [102] and Siz1 activity [83], influencing the DNA damage response; but it also regulates actin cytoskeleton dynamics [103], which affect many vital cellular functions such as transport, autophagy or cell division.

We think the data presented here bring us closer to understanding how the Rad51 level and function are regulated in response to genotoxic stress and also permit an initial look at this complex regulation circuit, which depends on Ub and SUMO ligases (Fig. 8). It is highly probable that each of these enzymes acts in certain circumstances. According to current knowledge concerning other substrates of these enzymes, we can anticipate the particular moments in the life of the cell when they play a major role in Rad51 regulation. Our findings and a growing amount of experimental data concerning PTMs of Rad51 recombinase homologs from different species indicate their crucial role in HR regulation. The existence of such inter-species similarities underlines the importance of the Rad51 PTMs network, suggesting it is evolutionarily conserved among all eukaryotes.

5. Conclusions

The significance of posttranslational modifications for protein functioning in vivo has been known for years; however, studies in recent years have provided increasing evidence that modifications with Ub and SUMO are crucial for regulating cellular processes that ensure a stable genome. Homologous recombination plays a significant role in genome maintenance, and Rad51 recombinase is one of the basic enzymes

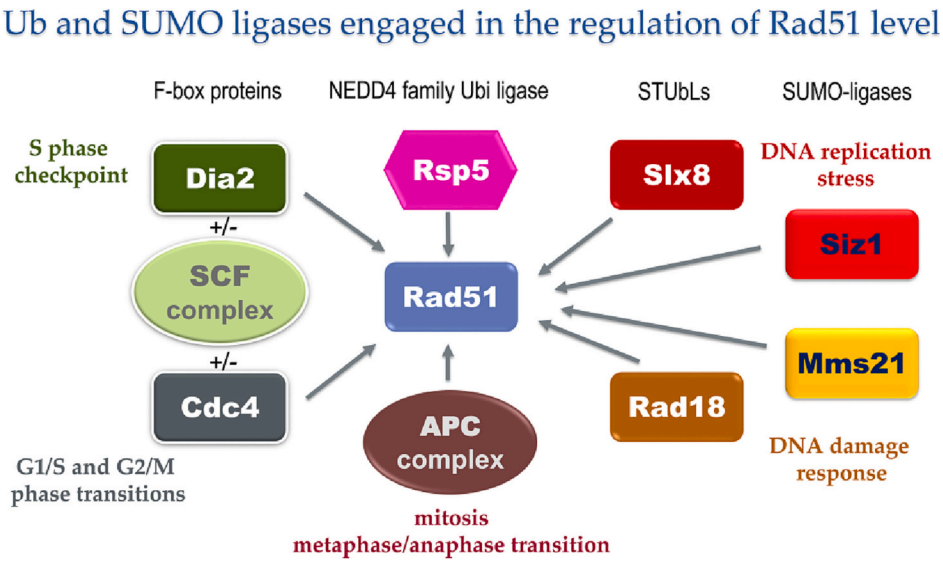

Fig. 8. Factors that contribute to Rad51 level regulation.
Ub and SUMO ligases engaged in PTMs of Rad51 recombinase, influencing Rad51 level and activity. The scheme is based on published data concerning other substrates of the presented enzymes. The moments in the cellular life when a certain enzyme modifies Rad51 are indicated.

involved in this DNA repair pathway. The Ub and SUMO, by modifying Rad51, change its cellular fate by deciding not only about its cellular level via dependent on these modifiers proteolysis but also influencing its function during DNA damage response through recruitment to DNA and removal from DNA. The Rad51 protein is able to form a filament on DNA, i.e., structure, vital for searching homologic sequences in DNA but also acts as an assembling platform stimulating the activity of the other proteins involved in the repair. Dysregulation of the E3 ligases enzymatic network that keeps Rad51 level and function under control likely leads to disruption in homologous recombination homeostasis, resulting in more frequent or illegitimate recombination, or perturbations in various DNA-linked processes (e.g., replication, transcription, or chromosome segregation) due to Rad51 filament that got immobilized on DNA persistently. All scenarios lead to harsh consequences, namely a drop in cell viability due to genomic instability or senescence due to blocked DNA transactions. Similar events in mammalian cells lead to disease development (e.g., genetic diseases and cancer) and aging.

Supplementary data to this article can be found online at https://doi.org/10.1016/j.bbamcr.2023.119526.

1. Abbreviations

APC	anaphase-promoting complex
CHX	cycloheximide
DSB	double-strand break
HR	homologous recombination
HRP	horseradish peroxidase
AP	alkaline phosphatase
PIC	phosphate inhibitor cocktail
poly-Ub	poly-ubiquitin
PTM	post-translational modification
RPA	replication protein A
SCF	Skp1-Cullin-F-box protein
STUbL	SUMO-targeted ubiquitin ligase
SUMO	small ubiquitin like modifier
Ub	ubiquitin
WB	western blot

CRediT authorship contribution statement

All authors contributed to the study conception and design. Material preparation, data collection and analysis were performed by Justyna Antoniuk-Majchrzak (strain construction, WB, affinity-isolation assay), Tuguldur Enkhbaatar (affinity-isolation assay, IP, WB, fluorescence microscopy), Anna Długajczyk (WB), Joanna Kaminska (affinity-isolation assay), Marek Skoneczny (IP), Daniel J. Klionsky (strains, antibodies), and Adrianna Skoneczna (strain and plasmid construction, WB, affinity-isolation assay, IP, sensitivity tests, flow cytometry). The first draft of the manuscript was written by Adrianna Skoneczna, Marek Skoneczny and Daniel J. Klionsky, all authors commented on previous versions of the manuscript. All authors read and approved the final manuscript.

Funding

This work was supported by the National Science Center grant 2016/21/B/NZ3/03641 and Institute of Biochemistry and Biophysics Polish Academy of Science grant DEC-MG-1/21-16 to A.S.

Ethics approval and consent to participate

Not applicable.

Consent for publication

Not applicable.

Declaration of competing interest

The authors declare that they have no known competing financial interests or personal relationships that could have appeared to influence the work reported in this paper.

Data availability

All data generated or analyzed during this study are included in this published article and its supplementary information files.

Acknowledgments

We thank Brenda J. Andrews, Ryszard Korona and Ewa Śledziewska-Gójska for strains, and Helle D. Ulrich, Teresa Żołądek, and Stephen P. Jackson for plasmids.

References

[1] A. Shinohara, H. Ogawa, T. Ogawa, Rad51 protein involved in repair and recombination in S. cerevisiae is a RecA-like protein, Cell 69 (1992) 457–470, https://doi.org/10.1016/0092-8674(92)90447-k.
[2] Z. Chen, H. Yang, N.P. Pavletich, Mechanism of homologous recombination from the RecA-ssDNA/dsDNA structures, Nature 453 (2008), https://doi.org/10.1038/nature06971 (489–484).
[3] T. Ogawa, X. Yu, A. Shinohara, E.H. Egelman, Similarity of the yeast RAD51 filament to the bacterial RecA filament, Science 259 (1993) 1896–1899, https://doi.org/10.1126/science.8456314.
[4] X. Yu, S.A. Jacobs, S.C. West, T. Ogawa, E.H. Egelman, Domain structure and dynamics in the helical filaments formed by RecA and Rad51 on DNA, Proc. Natl. Acad. Sci. U. S. A. 98 (2001) 8419–8424, https://doi.org/10.1073/pnas.111005398.
[5] E.M. Tavares, W.D. Wright, W.-D. Heyer, E. Le Cam, P. Dupaigne, In vitro role of Rad54 in Rad51-ssDNA filament-dependent homology search and synaptic complexes formation, Nat. Commun. 10 (2019) 4058, https://doi.org/10.1038/s41467-019-12082-z.
[6] C. Seong, S. Colavito, Y. Kwon, P. Sung, L. Krejci, Regulation of Rad51 recombinase presynaptic filament assembly via interactions with the Rad52 mediator and the Srs2 anti-recombinase, J. Biol. Chem. 284 (2009) 24363–24371, https://doi.org/10.1074/jbc.M109.032953.
[7] A. Shinohara, H. Ogawa, Y. Matsuda, N. Ushio, K. Ikeo, T. Ogawa, Cloning of human, mouse and fission yeast recombination genes homologous to RAD51 and recA, Nat. Genet. 4 (1993) 239–243, https://doi.org/10.1038/ng0793-239.
[8] G.M. Manthey, A.M. Bailis, Rad51 inhibits translocation formation by non-conservative homologous recombination in saccharomyces cerevisiae, PLoS One 5 (2010), e11889, https://doi.org/10.1371/journal.pone.0011889.
[9] T.M. Kim, J.H. Ko, L. Hu, S.-A. Kim, A.J.R. Bishop, J. Vijg, C. Montagna, P. Hasty, RAD51 mutants cause replication defects and chromosomal instability, Mol. Cell. Biol. 32 (2012) 3663–3680, https://doi.org/10.1128/MCB.00406-12.
[10] T. Tsuzuki, Y. Fujii, K. Sakumi, Y. Tominaga, K. Nakao, M. Sekiguchi, A. Matsushiro, Y. Yoshimura, T. Morita, Targeted disruption of the Rad51 gene leads to lethality in embryonic mice, Proc. Natl. Acad. Sci. U. S. A. 93 (1996) 6236–6240, https://doi.org/10.1073/pnas.93.13.6236.
[11] M. Kato, K. Yano, F. Matsuo, H. Saito, T. Katagiri, H. Kurumizaka, M. Yoshimoto, F. Kasumi, F. Akiyama, G. Sakamoto, H. Nagawa, Y. Nakamura, Y. Miki, Identification of Rad51 alteration in patients with bilateral breast cancer, J. Hum. Genet. 45 (2000) 133–137, https://doi.org/10.1007/s100380050199.
[12] J. Chen, M.D. Morrical, K.A. Donigan, J.B. Weidhaas, J.B. Sweasy, A.M. Averill, J. A. Tomczak, S.W. Morrical, Tumor-associated mutations in a conserved structural motif alter physical and biochemical properties of human RAD51 recombinase, Nucleic Acids Res. 43 (2015) 1098–1111, https://doi.org/10.1093/nar/gku1337.
[13] A.T. Wang, T. Kim, J.E. Wagner, B.A. Conti, F.P. Lach, A.L. Huang, H. Molina, E. M. Sanborn, H. Zierhut, B.K. Cornes, A. Abhyankar, C. Sougnez, S.B. Gabriel, A. D. Auerbach, S.C. Kowalczykowski, A. Smogorzewska, A dominant mutation in human RAD51 reveals its function in DNA interstrand crosslink repair independent of homologous recombination, Mol. Cell 59 (2015) 478–490, https://doi.org/10.1016/j.molcel.2015.07.009.
[14] N. Ameziane, P. May, A. Haitjema, H.J. van de Vrugt, S.E. van Rossum-Fikkert, D. Ristic, G.J. Williams, J. Balk, D. Rockx, H. Li, M.A. Rooimans, A.B. Oostra, E. Velleuer, R. Dietrich, O.B. Bleijerveld, A.F. Maarten Altelaar, H. Meijers-Heijboer, H. Joenje, G. Glusman, J. Roach, L. Hood, D. Galas, C. Wyman, R. Balling, J. den Dunnen, J.P. de Winter, R. Kanaar, R. Gelinas, J.C. Dorsman, A novel Fanconi anaemia subtype associated with a dominant-negative mutation in RAD51, Nat. Commun. 6 (2015) 8829, https://doi.org/10.1038/ncomms9829.
[15] M.J. Neale, S. Keeney, Clarifying the mechanics of DNA strand exchange in meiotic recombination, Nature 442 (2006) 153–158, https://doi.org/10.1038/nature04885.
[16] J.P. Lao, V. Cloud, C.-C. Huang, J. Grubb, D. Thacker, C.-Y. Lee, M.E. Dresser, N. Hunter, D.K. Bishop, Meiotic crossover control by concerted action of Rad51-

Dmc1 in homolog template bias and robust homeostatic regulation, PLoS Genet. 9 (2013), e1003978, https://doi.org/10.1371/journal.pgen.1003978.
[17] M.S. Brown, D.K. Bishop, DNA strand exchange and RecA homologs in meiosis, Cold Spring Harb. Perspect. Biol. 7 (2014), a016659, https://doi.org/10.1101/cshperspect.a016659.
[18] G. Lim, Y. Chang, W.-K. Huh, Phosphoregulation of Rad51/Rad52 by CDK1 functions as a molecular switch for cell cycle–specific activation of homologous recombination, Sci. Adv. 6 (2020) eaay2669, https://doi.org/10.1126/sciadv.aay2669.
[19] S. Flott, Y. Kwon, Y.Z. Pigli, P.A. Rice, P. Sung, S.P. Jackson, Regulation of Rad51 function by phosphorylation, EMBO Rep. 12 (2011) 833–839, https://doi.org/10.1038/embor.2011.127.
[20] Cyclebase 3.0 - RAD51, (n.d.). https://cyclebase.org/CyclebasePage?type=4932&id=YER095W (accessed January 13, 2020).
[21] E. Caba, D.A. Dickinson, G.R. Warnes, J. Aubrecht, Differentiating mechanisms of toxicity using global gene expression analysis in Saccharomyces cerevisiae, Mutat. Res. 575 (2005) 34–46, https://doi.org/10.1016/j.mrfmmm.2005.02.005.
[22] K. Krol, J. Antoniuk-Majchrzak, M. Skoneczny, M. Sienko, J. Jendrysek, I. Rumienczyk, A. Halas, A. Kurlandzka, A. Skoneczna, Lack of G1/S control destabilizes the yeast genome via replication stress-induced DSBs and illegitimate recombination, J. Cell Sci. 131 (2018) jcs226480, https://doi.org/10.1242/jcs.226480.
[23] G. Giaever, A.M. Chu, L. Ni, C. Connelly, L. Riles, S. Véronneau, S. Dow, A. Lucau-Danila, K. Anderson, B. André, A.P. Arkin, A. Astromoff, M. El-Bakkoury, R. Bangham, R. Benito, S. Brachat, S. Campanaro, M. Curtiss, K. Davis, A. Deutschbauer, K.-D. Entian, P. Flaherty, F. Foury, D.J. Garfinkel, M. Gerstein, D. Gotte, U. Güldener, J.H. Hegemann, S. Hempel, Z. Herman, D.F. Jaramillo, D. E. Kelly, S.L. Kelly, P. Kötter, D. LaBonte, D.C. Lamb, N. Lan, H. Liang, H. Liao, L. Liu, C. Luo, M. Lussier, R. Mao, P. Menard, S.L. Ooi, J.L. Revuelta, C.J. Roberts, M. Rose, P. Ross-Macdonald, B. Scherens, G. Schimmack, B. Shafer, D. D. Shoemaker, S. Sookhai-Mahadeo, R.K. Storms, J.N. Strathern, G. Valle, M. Voet, G. Volckaert, C. Wang, T.R. Ward, J. Wilhelmy, E.A. Winzeler, Y. Yang, G. Yen, E. Youngman, K. Yu, H. Bussey, J.D. Boeke, M. Snyder, P. Philippsen, R. W. Davis, M. Johnston, Functional profiling of the Saccharomyces cerevisiae genome, Nature 418 (2002) 387–391, https://doi.org/10.1038/nature00935.
[24] Z. Li, F.J. Vizeacoumar, S. Bahr, J. Li, J. Warringer, F.S. Vizeacoumar, R. Min, B. Vandersluis, J. Bellay, M. Devit, J.A. Fleming, A. Stephens, J. Haase, Z.-Y. Lin, A. Baryshnikova, H. Lu, Z. Yan, K. Jin, S. Barker, A. Datti, G. Giaever, C. Nislow, C. Bulawa, C.L. Myers, M. Costanzo, A.-C. Gingras, Z. Zhang, A. Blomberg, K. Bloom, B. Andrews, C. Boone, Systematic exploration of essential yeast gene function with temperature-sensitive mutants, Nat. Biotechnol. 29 (2011) 361–367, https://doi.org/10.1038/nbt.1832.
[25] A. Halas, M. Krawczyk, E. Sledziewska-Gojska, PCNA SUMOylation protects against PCNA polyubiquitination-mediated, Rad59-dependent, spontaneous, intrachromosomal gene conversion, in: Mutation Research/Fundamental and Molecular Mechanisms of Mutagenesis 791–792, 2016, pp. 10–18, https://doi.org/10.1016/j.mrfmmm.2016.08.001.
[26] J. McIntyre, A. Podlaska, A. Skoneczna, A. Halas, E. Sledziewska-Gojska, Analysis of the spontaneous mutator phenotype associated with 20S proteasome deficiency in S. cerevisiae, Mutat. Res. 593 (2006) 153–163, https://doi.org/10.1016/j.mrfmmm.2005.07.003.
[27] R.S. Sikorski, P. Hieter, A system of shuttle vectors and yeast host strains designed for efficient manipulation of DNA in Saccharomyces cerevisiae, Genetics 122 (1989) 19–27.
[28] C. Taxis, M. Knop, System of centromeric, episomal, and integrative vectors based on drug resistance markers for Saccharomyces cerevisiae, BioTechniques 40 (2006) 73–78.
[29] W.P. Voth, Y.W. Jiang, D.J. Stillman, New “marker swap” plasmids for converting selectable markers on budding yeast gene disruptions and plasmids, Yeast 20 (2003) 985–993, https://doi.org/10.1002/yea.1018.
[30] J.L. Parker, H.D. Ulrich, A SUMO-interacting motif activates budding yeast ubiquitin ligase Rad18 towards SUMO-modified PCNA, Nucleic Acids Res. 40 (2012) 11380–11388, https://doi.org/10.1093/nar/gks892.
[31] E. Garí, L. Piedrafita, M. Aldea, E. Herrero, A set of vectors with a tetracycline-regulatable promoter system for modulated gene expression in Saccharomyces cerevisiae, Yeast 13 (1997) 837–848, https://doi.org/10.1002/(SICI)1097-0061(199707)13:9<837::AID-YEA145>3.0.CO;2-T.
[32] K. Jarmoszewicz, K. Łukasiak, H. Riezman, J. Kaminska, Rsp5 ubiquitin ligase is required for protein trafficking in Saccharomyces cerevisiae COPI mutants, PLoS One 7 (2012), e39582, https://doi.org/10.1371/journal.pone.0039582.
[33] M. Stawiecka-Mirota, W. Pokrzywa, J. Morvan, T. Zoladek, R. Haguenauer-Tsapis, D. Urban-Grimal, P. Morsomme, Targeting of Sna3p to the endosomal pathway depends on its interaction with Rsp5p and multivesicular body sorting on its ubiquitylation, Traffic 8 (2007) 1280–1296, https://doi.org/10.1111/j.1600-0854.2007.00610.x.
[34] M. Hochstrasser, M.J. Ellison, V. Chau, A. Varshavsky, The short-lived MAT alpha 2 transcriptional regulator is ubiquitinated in vivo, Proc. Natl. Acad. Sci. U. S. A. 88 (1991) 4606–4610, https://doi.org/10.1073/pnas.88.11.4606.
[35] H.D. Ulrich, A.A. Davies, In vivo detection and characterization of sumoylation targets in Saccharomyces cerevisiae, Methods Mol. Biol. 497 (2009) 81–103, https://doi.org/10.1007/978-1-59745-566-4_6.
[36] A.A. Davies, H.D. Ulrich, Detection of PCNA modifications in Saccharomyces cerevisiae, Methods Mol. Biol. 920 (2012) 543–567, https://doi.org/10.1007/978-1-61779-998-3_36.
[37] M. Lisby, J.H. Barlow, R.C. Burgess, R. Rothstein, Choreography of the DNA damage response: spatiotemporal relationships among checkpoint and repair proteins, Cell 118 (2004) 699–713, https://doi.org/10.1016/j.cell.2004.08.015.
[38] D.M. Gelperin, M.A. White, M.L. Wilkinson, Y. Kon, L.A. Kung, K.J. Wise, N. Lopez-Hoyo, L. Jiang, S. Piccirillo, H. Yu, M. Gerstein, M.E. Dumont, E. M. Phizicky, M. Snyder, E.J. Grayhack, Biochemical and genetic analysis of the yeast proteome with a movable ORF collection, Genes Dev. 19 (2005) 2816–2826, https://doi.org/10.1101/gad.1362105.
[39] C. Stringer, T. Wang, M. Michaelos, M. Pachitariu, Cellpose: a generalist algorithm for cellular segmentation, Nat. Methods 18 (2021) 100–106, https://doi.org/10.1038/s41592-020-01018-x.
[40] J. Schindelin, I. Arganda-Carreras, E. Frise, V. Kaynig, M. Longair, T. Pietzsch, S. Preibisch, C. Rueden, S. Saalfeld, B. Schmid, J.-Y. Tinevez, D.J. White, V. Hartenstein, K. Eliceiri, P. Tomancak, A. Cardona, Fiji: an open-source platform for biological-image analysis, Nat. Methods 9 (2012) 676–682, https://doi.org/10.1038/nmeth.2019.
[41] D. Legland, I. Arganda-Carreras, P. Andrey, MorphoLibJ: integrated library and plugins for mathematical morphology with ImageJ, Bioinformatics 32 (2016) 3532–3534, https://doi.org/10.1093/bioinformatics/btw413.
[42] S. Berg, D. Kutra, T. Kroeger, C.N. Straehle, B.X. Kausler, C. Haubold, M. Schiegg, J. Ales, T. Beier, M. Rudy, K. Eren, J.I. Cervantes, B. Xu, F. Beuttenmueller, A. Wolny, C. Zhang, U. Koethe, F.A. Hamprecht, A. Kreshuk, ilastik: interactive machine learning for (bio)image analysis, Nat. Methods 16 (2019) 1226–1232, https://doi.org/10.1038/s41592-019-0582-9.
[43] D.R. Stirling, M.J. Swain-Bowden, A.M. Lucas, A.E. Carpenter, B.A. Cimini, A. Goodman, CellProfiler 4: improvements in speed, utility and usability, BMC Bioinformatics 22 (2021) 433, https://doi.org/10.1186/s12859-021-04344-9.
[44] T. Kluyver, B. Ragan-Kelley, F. Pérez, B. Granger, M. Bussonnier, J. Frederic, K. Kelley, J. Hamrick, J. Grout, S. Corlay, P. Ivanov, D. Avila, S. Abdalla, C. Willing, in: F. Loizides, B. Scmidt (Eds.), Jupyter Development Team, Jupyter Notebooks – A Publishing Format for Reproducible Computational Workflows, IOS Press, 2016, pp. 87–90, https://doi.org/10.3233/978-1-61499-649-1-87.
[45] W. McKinney, Data Structures for Statistical Computing in Python, 2010, https://doi.org/10.25080/majora-92bf1922-00a.
[46] P. Virtanen, R. Gommers, T.E. Oliphant, M. Haberland, T. Reddy, D. Cournapeau, E. Burovski, P. Peterson, W. Weckesser, J. Bright, S.J. van der Walt, M. Brett, J. Wilson, K.J. Millman, N. Mayorov, A.R.J. Nelson, E. Jones, R. Kern, E. Larson, C.J. Carey, İ. Polat, Y. Feng, E.W. Moore, J. VanderPlas, D. Laxalde, J. Perktold, R. Cimrman, I. Henriksen, E.A. Quintero, C.R. Harris, A.M. Archibald, A. H. Ribeiro, F. Pedregosa, P. van Mulbregt, SciPy 1.0 Contributors, SciPy 1.0: fundamental algorithms for scientific computing in Python, Nat. Methods 17 (2020) 261–272, https://doi.org/10.1038/s41592-019-0686-2.
[47] R. Zadrag-Tecza, A. Skoneczna, Reproductive potential and instability of the rDNA region of the Saccharomyces cerevisiae yeast: common or separate mechanisms of regulation? Exp. Gerontol. 84 (2016) 29–39, https://doi.org/10.1016/j.exger.2016.08.009.
[48] R. Zadrag-Tecza, M. Kwolek-Mirek, M. Alabrudzinska, A. Skoneczna, Cell size influences the reproductive potential and total lifespan of the Saccharomyces cerevisiae yeast as revealed by the analysis of polyploid strains, Oxidative Med. Cell. Longev. 2018 (2018) 1898421, https://doi.org/10.1155/2018/1898421.
[49] W. Heinemeyer, M. Fischer, T. Krimmer, U. Stachon, D.H. Wolf, The active sites of the eukaryotic 20 S proteasome and their involvement in subunit precursor processing, J. Biol. Chem. 272 (1997) 25200–25209, https://doi.org/10.1074/jbc.272.40.25200.
[50] J. McIntyre, H. Baranowska, A. Skoneczna, A. Halas, E. Sledziewska-Gojska, The spectrum of spontaneous mutations caused by deficiency in proteasome maturase Ump1 in Saccharomyces cerevisiae, Curr. Genet. 52 (2007) 221–228, https://doi.org/10.1007/s00294-007-0156-8.
[51] P.C. Ramos, J. Höckendorff, E.S. Johnson, A. Varshavsky, R.J. Dohmen, Ump1p is required for proper maturation of the 20S proteasome and becomes its substrate upon completion of the assembly, Cell 92 (1998) 489–499, https://doi.org/10.1016/S0092-8674(00)80942-3.
[52] T. Hanada, Y. Ohsumi, Structure-function relationship of Atg12, a ubiquitin-like modifier essential for autophagy, Autophagy 1 (2005) 110–118, https://doi.org/10.4161/auto.1.2.1858.
[53] G.A.G. Dittmar, C.R.M. Wilkinson, P.T. Jedrzejewski, D. Finley, Role of a ubiquitin-like modification in polarized morphogenesis, Science 295 (2002) 2442–2446, https://doi.org/10.1126/science.1069989.
[54] J. Lüders, G. Pyrowolakis, S. Jentsch, The ubiquitin-like protein HUB1 forms SDS-resistant complexes with cellular proteins in the absence of ATP, EMBO Rep. 4 (2003) 1169–1174, https://doi.org/10.1038/sj.embor.7400025.
[55] D. Liakopoulos, G. Doenges, K. Matuschewski, S. Jentsch, A novel protein modification pathway related to the ubiquitin system, EMBO J. 17 (1998) 2208–2214, https://doi.org/10.1093/emboj/17.8.2208.
[56] A.S. Goehring, D.M. Rivers, G.F. Sprague, Urmylation: a ubiquitin-like pathway that functions during invasive growth and budding in yeast, Mol. Biol. Cell 14 (2003) 4329–4341, https://doi.org/10.1091/mbc.e03-02-0079.
[57] Y. Takahashi, A. Toh-e, Y. Kikuchi, A novel factor required for the SUMO1/Smt3 conjugation of yeast septins, Gene 275 (2001) 223–231, https://doi.org/10.1016/s0378-1119(01)00662-x.
[58] E.S. Johnson, A.A. Gupta, An E3-like factor that promotes SUMO conjugation to the yeast septins, Cell 106 (2001) 735–744, https://doi.org/10.1016/s0092-8674(01)00491-3.
[59] M.-E. Serrentino, E. Chaplais, V. Sommermeyer, V. Borde, Differential association of the conserved SUMO ligase Zip3 with meiotic double-strand break sites reveals

regional variations in the outcome of meiotic recombination, PLoS Genet. 9 (2013), e1003416, https://doi.org/10.1371/journal.pgen.1003416.
[60] C.-H. Cheng, Y.-H. Lo, S.-S. Liang, S.-C. Ti, F.-M. Lin, C.-H. Yeh, H.-Y. Huang, T.-F. Wang, SUMO modifications control assembly of synaptonemal complex and polycomplex in meiosis of Saccharomyces cerevisiae, Genes Dev. 20 (2006) 2067–2081, https://doi.org/10.1101/gad.1430406.
[61] X. Zhao, G. Blobel, A SUMO ligase is part of a nuclear multiprotein complex that affects DNA repair and chromosomal organization, Proc. Natl. Acad. Sci. U. S. A. 102 (2005) 4777–4782, https://doi.org/10.1073/pnas.0500537102.
[62] S.R. Santa Maria, V. Gangavarapu, R.E. Johnson, L. Prakash, S. Prakash, Requirement of Nse1, a subunit of the Smc5-Smc6 complex, for Rad52-dependent postreplication repair of UV-damaged DNA in Saccharomyces cerevisiae, Mol. Cell. Biol. 27 (2007) 8409–8418, https://doi.org/10.1128/MCB.01543-07.
[63] C. Horigome, D.E. Bustard, I. Marcomini, N. Delgoshaie, M. Tsai-Pflugfelder, J. A. Cobb, S.M. Gasser, PolySUMOylation by Siz2 and Mms21 triggers relocation of DNA breaks to nuclear pores through the Slx5/Slx8 STUbL, Genes Dev. 30 (2016) 931–945, https://doi.org/10.1101/gad.277665.116.
[64] T. Srikumar, M.C. Lewicki, M. Costanzo, J.M. Tkach, H. van Bakel, K. Tsui, E. S. Johnson, G.W. Brown, B.J. Andrews, C. Boone, G. Giaever, C. Nislow, B. Raught, Global analysis of SUMO chain function reveals multiple roles in chromatin regulation, J. Cell Biol. 201 (2013) 145–163, https://doi.org/10.1083/jcb.201210019.
[65] F.R. Papa, M. Hochstrasser, The yeast DOA4 gene encodes a deubiquitinating enzyme related to a product of the human tre-2 oncogene, Nature 366 (1993) 313–319, https://doi.org/10.1038/366313a0.
[66] J.R. Mullen, C.-F. Chen, S.J. Brill, Wss1 is a SUMO-dependent isopeptidase that interacts genetically with the Slx5-Slx8 SUMO-targeted ubiquitin ligase, Mol. Cell. Biol. 30 (2010) 3737–3748, https://doi.org/10.1128/MCB.01649-09.
[67] D. Blake, B. Luke, P. Kanellis, P. Jorgensen, T. Goh, S. Penfold, B.-J. Breitkreutz, D. Durocher, M. Peter, M. Tyers, The F-box protein Dia2 overcomes replication impedance to promote genome stability in Saccharomyces cerevisiae, Genetics 174 (2006) 1709–1727, https://doi.org/10.1534/genetics.106.057836.
[68] J. Kaminska, M. Spiess, M. Stawiecka-Mirota, R. Monkaityte, R. Haguenauer-Tsapis, D. Urban-Grimal, B. Winsor, T. Zoladek, Yeast Rsp5 ubiquitin ligase affects the actin cytoskeleton in vivo and in vitro, Eur. J. Cell Biol. 90 (2011) 1016–1028, https://doi.org/10.1016/j.ejcb.2011.08.002.
[69] F. Cardona, A. Aranda, M. del Olmo, Ubiquitin ligase Rsp5p is involved in the gene expression changes during nutrient limitation in Saccharomyces cerevisiae, Yeast 26 (2009) 1–15, https://doi.org/10.1002/yea.1645.
[70] P.P. Shah, X. Zheng, A. Epshtein, J.N. Carey, D.K. Bishop, H.L. Klein, Swi2/Snf2-related translocases prevent accumulation of toxic Rad51 complexes during mitotic growth, Mol. Cell 39 (2010) 862–872, https://doi.org/10.1016/j.molcel.2010.08.028.
[71] T. Wagner, L. Pérez-Martínez, R. Schellhaas, M. Barrientos-Moreno, M. Öztürk, F. Prado, F. Butter, B. Luke, Chromatin modifiers and recombination factors promote a telomere fold-back structure, that is lost during replicative senescence, PLoS Genet. 16 (2020), e1008603, https://doi.org/10.1371/journal.pgen.1008603.
[72] E. Sonoda, M.S. Sasaki, J.M. Buerstedde, O. Bezzubova, A. Shinohara, H. Ogawa, M. Takata, Y. Yamaguchi-Iwai, S. Takeda, Rad51-deficient vertebrate cells accumulate chromosomal breaks prior to cell death, EMBO J. 17 (1998) 598–608, https://doi.org/10.1093/emboj/17.2.598.
[73] T.K. Foo, B. Xia, BRCA1-dependent and independent recruitment of PALB2-BRCA2-RAD51 in the DNA damage response and cancer, Cancer Res. 82 (2022) 3191–3197, https://doi.org/10.1158/0008-5472.CAN-22-1535.
[74] P. Tennstedt, R. Fresow, R. Simon, A. Marx, L. Terracciano, C. Petersen, G. Sauter, E. Dikomey, K. Borgmann, RAD51 overexpression is a negative prognostic marker for colorectal adenocarcinoma, Int. J. Cancer 132 (2013) 2118–2126, https://doi.org/10.1002/ijc.27907.
[75] H.L. Klein, The consequences of Rad51 overexpression for normal and tumor cells, DNA Repair (Amst) 7 (2008) 686–693, https://doi.org/10.1016/j.dnarep.2007.12.008.
[76] G. Bennett, M. Papamichos-Chronakis, C.L. Peterson, DNA repair choice defines a common pathway for recruitment of chromatin regulators, Nat. Commun. 4 (2013) 2084, https://doi.org/10.1038/ncomms3084.
[77] T.-T. Woo, C.-N. Chuang, M. Higashide, A. Shinohara, T.-F. Wang, Dual roles of yeast Rad51 N-terminal domain in repairing DNA double-strand breaks, Nucleic Acids Res. 48 (2020) 8474–8489, https://doi.org/10.1093/nar/gkaa587.
[78] K. Drabikowski, J. Ferralli, M. Kistowski, J. Oledzki, M. Dadlez, R. Chiquet-Ehrismann, Comprehensive list of SUMO targets in Caenorhabditis elegans and its implication for evolutionary conservation of SUMO signaling, Sci. Rep. 8 (2018) 1139, https://doi.org/10.1038/s41598-018-19424-9.
[79] S. Inano, K. Sato, Y. Katsuki, W. Kobayashi, H. Tanaka, K. Nakajima, S. Nakada, H. Miyoshi, K. Knies, A. Takaori-Kondo, D. Schindler, M. Ishiai, H. Kurumizaka, M. Takata, RFWD3-mediated ubiquitination promotes timely removal of both RPA and RAD51 from DNA damage sites to facilitate homologous recombination, Mol. Cell 66 (2017) 622–634.e8, https://doi.org/10.1016/j.molcel.2017.04.022.
[80] J. Muraszko, K. Kramarz, B. Argunhan, K. Ito, G. Baranowska, Y. Kurokawa, Y. Murayama, H. Tsubouchi, S. Lambert, H. Iwasaki, D. Dziadkowiec, Rrp1 translocase and ubiquitin ligase activities restrict the genome destabilising effects of Rad51 in fission yeast, Nucleic Acids Res. 49 (2021) 6832–6848, https://doi.org/10.1093/nar/gkab511.
[81] C. Hoege, B. Pfander, G.-L. Moldovan, G. Pyrowolakis, S. Jentsch, RAD6-dependent DNA repair is linked to modification of PCNA by ubiquitin and SUMO, Nature 419 (2002) 135–141, https://doi.org/10.1038/nature00991.
[82] A. Skoneczna, M. Skoneczny, Mitotic genome variation in yeast and other fungi, in: Somatic Genome Variation: In Animals, Plants, and Microorganisms, John Wiley & Sons, 2017.
[83] T.V. Novoselova, R.-S. Rose, H.M. Marks, J.A. Sullivan, SUMOylation regulates the homologous to E6-AP carboxyl terminus (HECT) ubiquitin ligase Rsp5p, J. Biol. Chem. 288 (2013) 10308–10317, https://doi.org/10.1074/jbc.M112.424234.
[84] G.A. Bauer, P.M. Burgers, Molecular cloning, structure and expression of the yeast proliferating cell nuclear antigen gene, Nucleic Acids Res. 18 (1990) 261–265, https://doi.org/10.1093/nar/18.2.261.
[85] L. Fan, T. Bi, L. Wang, W. Xiao, DNA-damage tolerance through PCNA ubiquitination and sumoylation, Biochem. J. 477 (2020) 2655–2677, https://doi.org/10.1042/BCJ20190579.
[86] M. Arbel, B. Liefshitz, M. Kupiec, DNA damage bypass pathways and their effect on mutagenesis in yeast, FEMS Microbiol. Rev. 45 (2021) fuaa038, https://doi.org/10.1093/femsre/fuaa038.
[87] J.L. Parker, H.D. Ulrich, SIM-dependent enhancement of substrate-specific SUMOylation by a ubiquitin ligase in vitro, Biochem. J. 457 (2014) 435–440, https://doi.org/10.1042/BJ20131381.
[88] B. Pfander, G.-L. Moldovan, M. Sacher, C. Hoege, S. Jentsch, SUMO-modified PCNA recruits Srs2 to prevent recombination during S phase, Nature 436 (2005) 428–433, https://doi.org/10.1038/nature03665.
[89] L. Krejci, S. Van Komen, Y. Li, J. Villemain, M.S. Reddy, H. Klein, T. Ellenberger, P. Sung, DNA helicase Srs2 disrupts the Rad51 presynaptic filament, Nature 423 (2003) 305–309, https://doi.org/10.1038/nature01577.
[90] Y. Xie, O. Kerscher, M.B. Kroetz, H.F. McConchie, P. Sung, M. Hochstrasser, The yeast Hex3.Slx8 heterodimer is a ubiquitin ligase stimulated by substrate sumoylation, J. Biol. Chem. 282 (2007) 34176–34184, https://doi.org/10.1074/jbc.M706025200.
[91] N.R. Bhagwat, S.N. Owens, M. Ito, J.V. Boinapalli, P. Poa, A. Ditzel, S. Kopparapu, M. Mahalawat, O.R. Davies, S.R. Collins, J.R. Johnson, N.J. Krogan, N. Hunter, SUMO is a pervasive regulator of meiosis, Elife 10 (2021), e57720, https://doi.org/10.7554/eLife.57720.
[92] D.L. Swaney, P. Beltrao, L. Starita, A. Guo, J. Rush, S. Fields, N.J. Krogan, J. Villén, Global analysis of phosphorylation and ubiquitylation cross-talk in protein degradation, Nat. Methods 10 (2013) 676–682, https://doi.org/10.1038/nmeth.2519.
[93] S. Back, A.W. Gorman, C. Vogel, G.M. Silva, Site-specific K63 ubiquitinomics provides insights into translation regulation under stress, J. Proteome Res. 18 (2019) 309–318, https://doi.org/10.1021/acs.jproteome.8b00623.
[94] D. Finley, H.D. Ulrich, T. Sommer, P. Kaiser, The ubiquitin–proteasome system of *Saccharomyces cerevisiae*, Genetics 192 (2012) 319–360, https://doi.org/10.1534/genetics.112.140467.
[95] A. Skoneczna, A. Kaniak, M. Skoneczny, Genetic instability in budding and fission yeast-sources and mechanisms, FEMS Microbiol. Rev. 39 (2015) 917–967, https://doi.org/10.1093/femsre/fuv028.
[96] T.S. Takahashi, H.-P. Wollscheid, J. Lowther, H.D. Ulrich, Effects of chain length and geometry on the activation of DNA damage bypass by polyubiquitylated PCNA, Nucleic Acids Res. 48 (2020) 3042–3052, https://doi.org/10.1093/nar/gkaa053.
[97] J.M. Whalen, N. Dhingra, L. Wei, X. Zhao, C.H. Freudenreich, Relocation of collapsed forks to the nuclear pore complex depends on sumoylation of DNA repair proteins and permits Rad51 association, Cell Rep. 31 (2020), 107635, https://doi.org/10.1016/j.celrep.2020.107635.
[98] R. Rai, S.P.M.V. Varma, N. Shinde, S. Ghosh, S.P. Kumaran, G. Skariah, S. Laloraya, Small ubiquitin-related modifier ligase activity of Mms21 is required for maintenance of chromosome integrity during the unperturbed mitotic cell division cycle in saccharomyces cerevisiae*, J. Biol. Chem. 286 (2011) 14516–14530, https://doi.org/10.1074/jbc.M110.157149.
[99] Y. Sun, L.M. Miller Jenkins, Y.P. Su, K.C. Nitiss, J.L. Nitiss, Y. Pommier, A conserved SUMO pathway repairs topoisomerase DNA-protein cross-links by engaging ubiquitin-mediated proteasomal degradation, Sci. Adv. 6 (2020), eaba6290, https://doi.org/10.1126/sciadv.aba6290.
[100] N. Serbyn, I. Bagdiul, A. Noireterre, A.H. Michel, R.T. Suhandynata, H. Zhou, B. Kornmann, F. Stutz, SUMO orchestrates multiple alternative DNA-protein crosslink repair pathways, Cell Rep. 37 (2021), 110034, https://doi.org/10.1016/j.celrep.2021.110034.
[101] G. Hariharasudhan, S.-Y. Jeong, M.-J. Kim, S.M. Jung, G. Seo, J.-R. Moon, S. Lee, I.-Y. Chang, Y. Kee, H.J. You, J.-H. Lee, TOPORS-mediated RAD51 SUMOylation facilitates homologous recombination repair, Nucleic Acids Res. 50 (2022) 1501–1516, https://doi.org/10.1093/nar/gkac009.
[102] N. Erdeniz, R. Rothstein, Rsp5, a ubiquitin-protein ligase, is involved in degradation of the single-stranded-DNA binding protein rfa1 in Saccharomyces cerevisiae, Mol. Cell. Biol. 20 (2000) 224–232, https://doi.org/10.1128/MCB.20.1.224-232.2000.
[103] J. Kamińska, B. Gajewska, A.K. Hopper, T. Zoładek, Rsp5p, a new link between the actin cytoskeleton and endocytosis in the yeast Saccharomyces cerevisiae, Mol. Cell. Biol. 22 (2002) 6946–6948, https://doi.org/10.1128/MCB.22.20.6946-6958.2002.